Physica A 602 (2022) 127646

Contents lists available at ScienceDirect

Physica A

journal homepage: www.elsevier.com/locate/physa

Lyapunov stability analysis and optimization measures for a dengue disease transmission model

Afeez Abidemi [a,*,1], Joseph Ackora-Prah [b,1], Hammed Olawale Fatoyinbo [c,1], Joshua Kiddy K. Asamoah [b,1]

[a] Department of Mathematical Sciences, Federal University of Technology, Akure, P.M.B. 704, Ondo State, Nigeria
[b] Department of Mathematics, Kwame Nkrumah University of Science and Technology, Kumasi, Ghana
[c] School of Mathematical and Computational Sciences, Massey University, Palmerston North, New Zealand

ARTICLE INFO

Article history:
Received 22 March 2022
Received in revised form 10 May 2022
Available online 2 June 2022

Keywords:
Dengue model
Optimal control theory
Sensitivity analysis
Lyapunov function
Cost-effectiveness analysis
Forward bifurcation

ABSTRACT

In this paper, we study a dengue model governed by an eight-dimensional autonomous system of ordinary differential equations using dynamical system theory. Appropriate Lyapunov functions are used to carry out an extensive investigation of the global asymptotic dynamics of the model around the dengue-free and dengue-present equilibria. The model is shown to exhibit a forward bifurcation phenomenon using Center Manifold Theory. Sensitivity analysis is carried out to determine the relative importance of the model parameters to the spread of the disease. Using optimal control theory, the model is further extended to a nonlinear optimal control model to explore the impact of four time-dependent control variables, namely, personal protection, treatment drug therapy for latently infected individuals, treatment control for symptomatic individuals and insecticide control for mosquito reduction, on dengue disease dynamics in a population. Cost-effectiveness analysis is conducted on various strategies with combinations of at least three optimal controls to determine the least costly and most effective strategy that can be implemented to contain the spread of dengue in a population.

1. Introduction

Dengue is one of the most important vector-borne diseases nowadays [1]. With the geographic distribution of the disease continuing to expand, dengue remains the leading cause of arthropod-borne viral disease globally [2,3]. It has dispersed almost all over the world [1]. Currently, dengue is endemic in at least 128 tropical and subtropical countries [3]. The disease has a vast impact on the economy of countries, especially where the disease is endemic [1]. Dengue is primarily caused by dengue virus (DENV), which can be subdivided into four distinct serotypes, namely, DENV-1, DENV-2, DENV-3 and DENV-4 [3–5]. The mosquito-borne viral pathogen (DENV) is transmitted by two species of mosquito, which are *Aedes aegypti* and *Aedes albopictus* [3,6]. *Aedes aegypti* mosquitoes are considered as the main vector for DENV transmission in urban regions, whereas *Aedes albopictus* mosquitoes are often found in peri-urban and rural environments [7].

Currently, more than 55% of the world's population live in areas at risk of dengue fever (DF) transmission [6], placing almost 3.9 billion people at risk of infection [3]. According to World Health Organization [8], there are about 50 million

* Corresponding author.
E-mail addresses: aabidemi@futa.edu.ng (A. Abidemi), ackoraprahj@gmail.com (J. Ackora-Prah), h.fatoyinbo@massey.ac.nz (H.O. Fatoyinbo), jkkasamoah@knust.edu.gh (J.K.K. Asamoah).

[1] All authors contributed equally to the development of this study and approved the final manuscript draft for submission.

https://doi.org/10.1016/j.physa.2022.127646
0378-4371/

to 100 million cases of DF and 500,000 cases of severe dengue, resulting in hundreds of thousands of hospitalizations and over 20,000 deaths, mostly among children and young adults each year. Over the past half century alone, the global prevalence of dengue has increased 30-fold, with a 500-fold increase in the most severe clinical manifestations such as dengue hemorrhagic fever (DHF) and dengue shock syndrome (DSS) [3].

DENV is transmitted from humans to vectors and from vectors to humans when a female *Aedes* mosquito bites an infected person and then bites another healthy individual [1,9]. The mosquitoes acquire infection from an infected person, then transmit the infection to other susceptible humans during blood meals [7]. The symptoms of dengue appear after 3–14 days of infected mosquito bite [4,6]. When a person is infected first time by a DENV, the immune response against that DENV is activated [6]. Recovery of such person from the primary dengue infection by one of the four DENV serotypes will acquire life-long immunity to the specific serotype but temporary cross-immunity to the remaining serotypes [4,10]. So, people who are reinfected with another serotype may experience antibody-dependent enhancement (ADE) in which the body's immune response exacerbates the clinical symptoms of dengue [9], and thereby at high risk of developing more severe diseases such as DHF and DSS [5].

Once infected, the typical symptoms of DF begin to develop over the incubation period [11]. The typical symptoms of this disease are identified by high fever, severe headache, pain behind the eyes, joint pains, nausea, vomiting [6,7], arthralgia, myalgia, rashes and others [11]. Though many of the cases end in uncomplicated DF, some may progress to a more severe form, namely, DHF which usually occurs soon after the end of the febrile phase and results in plasma leakage. If plasma leakage becomes severe, with hypovolemic shock, the disease may progress to DSS which is potentially fatal [11]. Failure to provide a timely medical treatment for any dengue-related human infections, particularly DHF and DSS, can lead to deaths [4]. It has been reported that the mortality of dengue is less than 0.4% [11].

As of now, there is no licenced therapeutic treatment or vaccine against dengue, although enormous efforts are in place to develop an actual vaccine [4,6,10]. Hospital treatment, which primarily relies on supportive care, is given only to encourage care like bed rest, antipyretics, analgesics and so on [6,12]. In particular, a live attenuated Dengvaxia vaccine, the chimeric yellow fever dengue virus tetravalent dengue vaccine (CYD-TDV), has been developed and licenced to be undertaken in dengue-endemic countries [13], including Thailand [13] and Indonesia [14] among others. However, aside from approving the vaccine only in countries where all the dengue virus serotypes co-circulating, a cautionary note that the vaccine should be given to individuals with prior dengue infections makes dengue vaccination programmes complicated. With this shortcomings, mosquito vector control and personal protection (precautionary measures) against mosquito bites remain the possible primary tools to fight against dengue [4,12]. This is primarily based on insecticides and community engagement for environmental management initiatives [12]. Insecticide-based control plays a major role among other dengue control activities [2].

The widespread of DENV can be linked to numerous factors, such as ineffective control strategies, geographically expanding *Aedes* mosquitoes, asymptomatic DENV-carrying humans movement on a large scale [7] and so on. So, numerous Mathematicians have developed models to analyse different aspects of dengue and other vector to human diseases for further understanding of the transmission dynamics and to influence the process of decision-making in respect of the intervention programmes for prevention and control of the diseases in a community in recent decades [15–21]. These include the vector-host interactions in homogeneous environments with the presence of a single DENV serotype [1,4,9,12,13,22–25], coexistence of two or more dengue virus serotypes [7,26–28], effects of human movements on the disease spread in a patchy environment [29,30], effects of seasonal variation [30,31] and within-host DENV transmission dynamics [6] among others. In particular, Sharma et al. [6] formulated and analysed a nonlinear mathematical model governed by an eight-dimensional system of ordinary differential equations describing the dynamics of T-cells and cytokines in dengue infection based on antiviral treatment to explore the interactions among dengue and body immune cells.

Abidemi et al. [27] developed and analysed a two-strain model to explore the impacts of administering Dengvaxia vaccine on seropositive individuals (that is, those who have previous health history of dengue infection and have recovered from at least primary infection before being vaccinated) and the use of vector control with constant rates of implementation on dengue transmission and control in a community. In another development, Abidemi et al. [26] studied the global asymptotic behaviour of a two-strain dengue model. The model was further extended to an optimal control model to evaluate how to effectively minimize the spread of dengue with the use of optimal Dengvaxia vaccine and insecticide control at a minimum cost.

In Knerer et al. [12], a mathematical model governed by an eleven-dimensional nonlinear system of ordinary differential equations describing the dynamics of transmission and control of dengue was developed and analysed. The model features the human population, *Wolbachia*-free mosquito population, *Wolbachia*-carrying mosquito population and vaccination control for the human population. In a similar work, Mentuda [23] studied different mathematical dengue models to compare the impacts of vaccination and vector control interventions in minimizing the number of dengue infections in the population. By extending the models to an optimal control problem, the study suggested that the healthy human population is better maximized in a short period using an optimal vector control than optimal vaccination. A nonlinear mathematical model incorporating vaccination administered on individuals after the primary infection is formulated and analysed to describe the dynamic of dengue by Chamnan et al. [13]. The authors further extended the model to an optimal control problem by incorporating two time-dependent control variables, namely, vaccination control and mosquito population control.

Brito da Cruz and Rodrigues [1] formulated and analysed a non-autonomous system of ordinary differential equations incorporating a time-dependent control function representing personal protective measures for optimal control of dengue disease transmission and spread. One insightful result arising from the study is that long protection may lead to the elimination of the disease in the population. Moreover, the idea of this study led Brito da Cruz and Rodrigues in [28] to propose a two-strain mathematical dengue model incorporating different personal protective measures with constant control rates and the effect of public awareness to the importance of using these personal protective measures. A key result arising from this study is that dengue can be prevented through human population perception to protect themselves from mosquito bites throughout the disease outbreak period.

In light of the result of sensitivity analysis conducted on the nonlinear mathematical model incorporating the effects of media awareness on dengue eradication programmes, Aldila [24] used the optimal control theory to analyse how three different control interventions, namely, media campaign policy, hospitalization control, and fumigation, affect the transmission dynamics of dengue. To determine the most cost-effective strategy to curtail the spread of the disease, the author carried out the cost-effectiveness analysis (CEA) on the intervention strategies. Similarly, Abidemi and Aziz [10] developed and analysed a nonlinear mathematical model for dengue disease transmission and control. Optimal control theory was employed for the qualitative analysis of the non-autonomous version of the model. Furthermore, the authors conducted CEA on different combinations of optimal personal protective intervention, larvicide and adulticide controls in stemming the spread of dengue in Malaysia.

A nonlinear mathematical model featuring the impact of information-based behavioural response and segregation of infected human population into detected and undetected population to assess the dynamics of transmission and control of dengue was proposed and discussed by Srivastav et al. [25]. The model was further extended to an optimal control problem by incorporating five time-dependent control variables accounting for intensity of behavioural response through information (protective measure), reduction of human–mosquito interaction control (protective measure), quarantine control for detected infected individuals, screening control for undetected infected individuals, and insecticide control for mosquito population reduction.

In [9], Asamoah et al. studied and analysed the global asymptotic behaviours of a seven-dimensional system of ordinary differential equations describing the transmission dynamics of dengue between the two interacting human and mosquito populations by constructing suitable Lyapunov functions. Further, the model was extended to an optimal control problem including four time-varying control variables representing insecticide-treated bed nets, vaccination, treatment (prophylactics) and insecticides. The authors conducted CEA on five different control combination strategies involving the use of at least two control measures to ascertain the least costly and most cost-effective control strategy.

Despite that the density of asymptomatic individuals (carriers) is higher than that of symptomatic individuals, with respective proportions of dengue-related infections [4,9], only few of the previous mathematical study considered the asymptomatic carriers of dengue infection [4,9,16]. For instance, Abidemi et al. [4] formulated and analysed the qualitative properties of solutions and existence of dengue-free equilibrium (DFE) of an eight-dimensional nonlinear mathematical dengue model incorporating asymptomatic (carrier) class and effects of four control interventions, namely, insecticide-treated bed nets (ITNs), treatment control for exposed individuals, treatment control for symptomatic individuals and insecticide control for mosquitoes, with constant rates. However, the authors did not determine the dengue-present equilibrium, examine the global asymptotic behaviours of the model around the dengue-free and dengue-present equilibria, and carry out global sensitivity analysis of the control reproduction number. Also, the optimal control version of the model was not studied, which did not allow for the economic evaluation of the control interventions considered in the study.

Motivated by the non-optimal control model presented in [4], we aim to study the global asymptotic dynamics of dengue, construct and analyse a nonlinear optimal control dengue model that captures asymptomatic class. Our nonlinear mathematical optimal control model, which is a modification of that of Abidemi and co-workers [4], is constructed to include four time-dependent control variables accounting for personal protection (with the use of ITNs or mosquito-repellent lotion), treatment drug therapy for latently infected individuals, treatment control for symptomatic individuals and insecticide control for mosquitoes. With the aid of suitably constructed Lyapunov functions, global asymptotic dynamics of the non-optimal control model is shown for both the DFE and dengue-present equilibrium (DPE). The new nonlinear optimal control dengue model is analysed using Pontryagin's maximum principle [32]. Numerical experiment is conducted to enhance the results arising from theoretical analysis. Lastly, CEA is carried out to determine the most cost-effective strategy for the minimization of dengue spread in the community using incremental cost-effectiveness ratio (ICER). This cost assessment can provide insightful information about the economic impact of dengue infections and can be used as a guide on how to prioritize control strategies for policy makers.

The following is how the rest of the paper is organized: A brief introduction to the formulation of the nonlinear mathematical model for dengue spread without optimal control is discussed in Section 2. Section 3 looks at the model's qualitative analysis. Numerical simulation of the model's global asymptotic stability and global sensitivity analysis is as well carried out in this section. In Section 4, the dengue model with optimal control is developed and its qualitative analysis is discussed in depth. In Section 5, numerical solution of the optimal control model is presented and the cost-effectiveness analysis results are also discussed in depth. The conclusion and final remarks are given in Section 6.

2. Dengue model without optimal control

Here, we give a brief introduction to the formulation of non-optimal control dengue model. In a previous study [4], Abidemi et al. presented and examined a compartmental mathematical model describing the transmission and control dynamics of dengue fever incorporating the effects of constant control rates, where the human and mosquito populations are stratified into five and three epidemiological classes respectively. The epidemiological classes for the total human population, denoted as $N_h(t)$, are susceptible humans (those who are prone to contract dengue infection), denoted as $S_h(t)$, exposed humans (those who have been infected without the disease symptoms), denoted as $E_h(t)$, asymptomatic humans (those that are not symptomatic but infectious), denoted as $A_h(t)$, symptomatic infectious humans (those who exhibit dengue symptoms and capable to spread the disease), denoted as $I_h(t)$, and recovered humans (those who are immune to the disease), denoted as $R_h(t)$. Thus, at any given time t,

$$N_h(t) = S_h(t) + E_h(t) + A_h(t) + I_h(t) + R_h(t).$$

While the total mosquito population, represented as $N_v(t)$, is grouped into susceptible mosquitoes ($S_v(t)$), exposed mosquitoes ($E_v(t)$) and infectious mosquitoes ($I_v(t)$). Consequently, the total mosquito population at any time t is expressed as

$$N_v(t) = S_v(t) + E_v(t) + I_v(t). \tag{1}$$

The dengue model governed by eight-dimensional nonlinear autonomous system of ordinary differential equations as proposed in [4] is presented as

$$\frac{dS_h}{dt} = \Lambda_h - \frac{b\beta_h(1-\varepsilon)S_hI_v}{N_h} - \mu_hS_h, \tag{2a}$$
$$\frac{dE_h}{dt} = \frac{b\beta_h(1-\varepsilon)S_hI_v}{N_h} - (\alpha_h + \mu_h)E_h, \tag{2b}$$
$$\frac{dA_h}{dt} = (1-\phi)\nu\alpha_hE_h - (\gamma_a + \mu_h)A_h, \tag{2c}$$
$$\frac{dI_h}{dt} = (1-\phi)(1-\nu)\alpha_hE_h - (\gamma_i + \tau_1\delta + \mu_h)I_h, \tag{2d}$$
$$\frac{dR_h}{dt} = \phi\alpha_hE_h + \gamma_aA_h + (\gamma_i + \tau_1\delta)I_h - \mu_hR_h, \tag{2e}$$
$$\frac{dS_v}{dt} = (1-\tau_2\xi)\Lambda_v - \frac{b\beta_v(1-\varepsilon)S_v(\eta A_h + I_h)}{N_h} - (\mu_v + \tau_2\xi)S_v, \tag{2f}$$
$$\frac{dE_v}{dt} = \frac{b\beta_v(1-\varepsilon)S_v(\eta A_h + I_h)}{N_h} - (\alpha_v + \mu_v + \tau_2\xi)E_v, \tag{2g}$$
$$\frac{dI_v}{dt} = \alpha_vE_v - (\mu_v + \tau_2\xi)I_v, \tag{2h}$$

subject to the initial conditions (ICs) given by

$$(S_h(0), E_h(0), A_h(0), I_h(0), R_h(0), S_v(0), E_v(0), I_v(0)) = (S_{0h}, E_{0h}, A_{0h}, I_{0h}, R_{0h}, S_{0v}, E_{0v}, I_{0v}). \tag{3}$$

The description and assumptions of model (2) are detailed in [4]. Here, the model parameters as described by the authors are reproduced in Table 1 for easy reference, while the modified schematic diagram of the dengue model (2) can be found in supplementary information.

3. Analysis of model (2)

3.1. Qualitative properties of solutions

3.1.1. Positivity of solutions

To establish the epidemiological meaningfulness of model (2), it was shown in [4] that the solutions of system (2) along with the non-negative ICs given in (3) remain non-negative for all time $t > 0$.

3.1.2. Invariant region

We study the solutions of model (2) in the closed set $\mathscr{D}$ given as

$$\mathscr{D} = \mathscr{D}_h \cup \mathscr{D}_v \subset \mathbb{R}^5_+ \times \mathbb{R}^3_+, \tag{4}$$

Table 1
Description of the parameters for dengue model (2).

Parameter	Description
Λ_h	Human recruitment rate
Λ_v	Mosquito recruitment rate
β_h	Transmission probability of dengue virus from I_v to S_h
μ_h	Human lifespan (per day)
b	Mosquito biting rate
β_v	Transmission probability of dengue virus from I_h and A_h to S_v
α_v	Disease progression rate of exposed mosquitoes to become infectious
μ_v	Lifespan of the female mosquitoes (per day)
ν	Fraction of new infectious humans that are asymptomatic
η	Modification parameter that accounts for the reduced infectiousness of humans in the A_h class when compared to humans in the I_h class
τ_1	Proportion of effective treatment
τ_2	Killing efficacy of adulticide control
α_h	Progression rate from either class A_h or I_h
α_v	Progression rate of mosquitoes to become infectious
γ_a	Progression rate from class A_h to class R_h
γ_i	Recovery rate of individuals in class I_h
ε	Personal protection using insecticide-treated bed nets (ITNs) or mosquito-repellent lotion
ϕ	Treatment drug therapy for latently infected humans, E_h
δ	Chemotherapy or treatment of individuals in class I_h
ξ	Mosquito reduction effort using open space spray of insecticide

with

$$\mathscr{D}_h = \left\{(S_h(t), E_h(t), A_h(t), I_h(t)R_h(t)) \in \mathbb{R}^5_+ : N_h(t) \leq \frac{\Lambda_h}{\mu_h}\right\},$$
$$\mathscr{D}_v = \left\{(S_v(t), E_v(t), I_v(t)) \in \mathbb{R}^3_+ : N_v(t) \leq \frac{\Lambda_v(1-\tau_2\xi)}{(\mu_v+\tau_2\xi)}\right\}.$$

In respect of model (2), the set $\mathscr{D}$ is positively invariant as previously carried out by Abidemi et al. in [4].

3.2. Existence of equilibria

Definition 3.1. An octuple $\mathscr{E} = (S_h, E_h, A_h, I_h, R_h, S_v, E_v, I_v) \in \mathbb{R}^8$ is said to be an equilibrium point of the system (2) if the derivatives of the right-hand of Eq. (2) is set to zero. Thus, the equilibrium point, $\mathscr{E}$, which is biologically meaningful whenever $\mathscr{E} \in \mathscr{D}$, is said to be a dengue-free equilibrium (DFE), denoted as $\mathscr{E}_f$, or dengue-present equilibrium (DPE), represented by $\mathscr{E}_p$, depending on E_h, A_h, I_h, E_v and I_v. If there is no disease in the interacting human and mosquito populations (i.e., $E_h = A_h = I_h = E_v = I_v = 0$), then $\mathscr{E}$ coincides with $\mathscr{E}_f$. Otherwise, if either $E_h > 0$, $A_h > 0$, $I_h > 0$, $E_v > 0$ or $I_v > 0$, then the equilibrium point $\mathscr{E}$ is called $\mathscr{E}_p$.

3.2.1. Dengue-free equilibrium

The dengue model (2) has a dengue-free equilibrium, $\mathscr{E}_f$, given by [4]

$$\mathscr{E}_f = \left(S_h^*, E_h^*, A_h^*, I_h^*, R_h^*, S_v^*, E_v^*, I_v^*\right) = \left(\frac{\Lambda_h}{\mu_h}, 0, 0, 0, 0, \frac{\Lambda_v(1-\xi)}{(\mu_v+\tau_2\xi)}, 0, 0\right). \tag{5}$$

Using the next-generation operator approach [33], the control (or effective) reproduction number, denoted as $\mathscr{R}_t$, of the dengue model (2) is computed in [4] as

$$\mathscr{R}_t = \sqrt{\frac{(1-\varepsilon)^2 b^2 \beta_h \beta_v (1-\phi)\alpha_h \mu_h (k_3\eta\nu + k_2(1-\nu))\alpha_v \Lambda_v (1-\xi)}{k_1 k_2 k_3 k_4 k_5 (\mu_v+\tau_2\xi)\Lambda_h}}, \tag{6}$$

where $k_1 = \alpha_h + \mu_h$, $k_2 = \gamma_a + \mu_h$, $k_3 = \gamma_i + \tau_1\delta + \mu_h$, $k_4 = \alpha_v + \mu_v + \tau_2\xi$ and $k_5 = \mu_v + \tau_2\xi$. The control reproduction number, $\mathscr{R}_t$, is used as an invasion threshold for both predicting dengue outbreaks and evaluating control strategies that would reduce the spread of dengue in the community. By lowering parameters that would increase the disease's spread, the control (effective) reproduction number will also reduce.

3.2.2. Dengue-present equilibrium

Let $\mathscr{E}_p = \left(S_h^{**}, E_h^{**}, A_h^{**}, I_h^{**}, R_h^{**}, S_v^{**}, E_v^{**}, I_v^{**}\right)$ denotes any arbitrary DPE of model (2). Further, let

$$\lambda_h^{**} = \frac{b\beta_h(1-\varepsilon)I_v^{**}}{N_h^{**}}, \tag{7a}$$

$$\lambda_v^{**} = \frac{b\beta_v(1-\varepsilon)(\eta A_h^{**} + I_h^{**})}{N_h^{**}}, \tag{7b}$$

where λ_h^{**} and λ_v^{**} represent the forces of infection of humans and mosquitoes at steady state respectively. Then, solving the system (2) with the right-hand set to zero yields

$$\left.\begin{aligned}
S_h^{**} &= \frac{\Lambda_h}{\lambda_h^{**}+\mu_h}, & S_v^{**} &= \frac{\Lambda_v(1-\tau_2\xi)}{(\lambda_v^{**}+k_5)},\\
E_h^{**} &= \frac{\Lambda_h\lambda_h^{**}}{k_1(\lambda_h^{**}+\mu_h)}, & E_v^{**} &= \frac{\Lambda_v(1-\tau_2\xi)\lambda_v^{**}}{k_4(\lambda_v^{**}+k_5)},\\
A_h^{**} &= \frac{k_7\Lambda_h\lambda_h^{**}}{k_1k_2(\lambda_h^{**}+\mu_h)}, & I_v^{**} &= \frac{\alpha_v\Lambda_v(1-\tau_2\xi)\lambda_v^{**}}{k_4k_5(\lambda_v^{**}+k_5)},\\
I_h^{**} &= \frac{k_8\Lambda_h\lambda_h^{**}}{k_1k_3(\lambda_h^{**}+\mu_h)},\\
R_h^{**} &= \frac{k_9\Lambda_h\lambda_h^{**}}{k_1k_2k_3\mu_h(\lambda_h^{**}+\mu_h)},
\end{aligned}\right\} \tag{8}$$

where $k_6 = \gamma_i + \tau_1\delta$, $k_7 = (1-\phi)\nu\alpha_h$, $k_8 = (1-\phi)(1-\nu)\alpha_h$.

Next, the two forces of infection in Eq. (7) are perturbed together.

Using A_h^{**}, I_h^{**} and I_v^{**} from Eq. (8) in Eq. (7), and after rigorous simplifications lead to the polynomial given as

$$p_0(\lambda_h^{**})^2 + p_1(\lambda_h^{**}) + p_2 = 0, \tag{9}$$

where,

$$\begin{aligned}
p_0 &= k_4k_5\Lambda_h(k_2k_3\mu_h + k_3k_7\mu_h + k_2k_8\mu_h + k_9)\\
&\quad\times [b\beta_v(1-\varepsilon)(k_3k_7\eta + k_2k_8)\mu_h + k_2k_3k_5\mu_h + k_3k_5k_7\mu_h + k_2k_5k_8\mu_h + k_5k_9], \qquad (10)\\
p_1 &= \{k_1k_2k_3k_4k_5\mu_h\Lambda_h[b\beta_v(1-\varepsilon)(k_3k_7\eta + k_2k_8)\mu_h + k_2k_3k_5\mu_h + k_3k_5k_7\mu_h + k_2k_5k_8\mu_h + k_5k_9]\\
&\quad + k_1k_2k_3k_4k_5^2\mu_h\Lambda_h(k_2k_3\mu_h + k_3k_7\mu_h + k_2k_8\mu_h + k_9)\\
&\quad - k_1k_2k_3b^2(1-\varepsilon)^2\beta_h\beta_v(k_3k_7\eta + k_2k_8)\mu_h^2\alpha_v\Lambda_v(1-\tau_2\xi)\}, \qquad (11)\\
p_2 &= k_1^2k_2^2k_3^2k_4k_5^2\mu_h^2\Lambda_h - k_1k_2k_3b^2(1-\varepsilon)^2\beta_h\beta_v(k_3k_7\eta + k_2k_8)\mu_h^3\alpha_v\Lambda_v(1-\tau_2\xi), \qquad (12)\\
p_2 &= k_1^2k_2^2k_3^2k_4k_5^2\mu_h^2\Lambda_h\left[1 - \frac{(1-\varepsilon)^2b^2\beta_h\beta_v(k_3k_7\eta + k_2k_8)\mu_h\alpha_v\Lambda_v(1-\tau_2\xi)}{k_1k_2k_3k_4k_5^2\Lambda_h}\right],\\
p_2 &= k_1^2k_2^2k_3^2k_4k_5^2\mu_h^2\Lambda_h\left(1-\mathscr{R}_t^2\right), \qquad (13)
\end{aligned}$$

and $k_9 = k_2k_3\phi\alpha_h + k_3k_7\gamma_a + k_2k_6k_8$. It is clear from Eq. (9) that p_0 is positive, and p_2 is positive whenever $\mathscr{R}_t < 1$ and negative whenever $\mathscr{R}_t > 1$. Thus, we claim the following result in Theorem 3.1.

Theorem 3.1. *The dengue model (2) has:*

(i) a unique DPE if and only if $p_2 < 0$ and $\mathscr{R}_t > 1$;
(ii) a unique DPE if $p_1 < 0$, and $p_2 = 0$ or $p_1^2 - 4p_0p_2 = 0$;
(iii) two DPE points if $p_2 > 0$, $p_1 < 0$ and $p_1^2 - 4p_0p_2 > 0$;
(iv) no DPE otherwise.

In Theorem 3.1, case (i) obviously shows that the dengue model (2) has a unique DPE whenever $\mathscr{R}_t > 1$. Furthermore, case (iii) of Theorem 3.1 shows the possibility of backward bifurcation whenever $\mathscr{R}_t < 1$. To show this possibility, we set the polynomial $p_1^2 - 4p_0p_2 = 0$, and solve for the critical values of $\mathscr{R}_t$, denoted by $\tilde{\mathscr{R}}_t$. Thus, $\tilde{\mathscr{R}}_t$ is given as

$$\tilde{\mathscr{R}}_t = \sqrt{1 - \frac{p_1^2}{4p_0k_1^2k_2^2k_3^2k_4k_5^2\mu_h^2\Lambda_h}}. \tag{14}$$

So, the dengue model (2) can exhibit backward bifurcation for the values of $\mathscr{R}_t$ such that $\tilde{\mathscr{R}}_t < \mathscr{R}_t < \mathscr{R}_0 < 1$, where $\mathscr{R}_0$ is the basic reproduction number derived from the expression $\mathscr{R}_t$ in (6) as

$$\mathscr{R}_0 = \sqrt{\frac{b^2\beta_h\beta_v\alpha_h\mu_h(\eta\nu(\gamma_i+\mu_h) + k_2(1-\nu))\alpha_v\Lambda_v}{k_1k_2(\gamma_i+\mu_h)\mu_v^2(\alpha_v+\mu_v)\Lambda_h}}. \tag{15}$$

3.2.3. Existence of forward bifurcation

Proof. From the model Eqs. (2a)–(2h), the following variables can be defined: $z_1^* = S_h, z_2^* = E_h, z_3^* = A_h, z_4^* = I_h, z_5^* = R_h, z_6^* = S_v, z_7^* = E_v$ and $z_8^* = I_v$. Hence, $N_h(t) = z_1^* + z_2^* + z_3^*, + z_4^* + z_5^*$ and $N_v(t) = z_6^* + z_7^* + z_8^*$. Now, using the vector notation $z^* = (z_1^*, z_2^*, z_3^*, z_4^*, z_5^*, z_6^*, z_7^*, z_8^*)^{T^*}$, the model Eqs. (2a)–(2h) can be written as $\frac{dz^*}{dt} := F = (f_1, f_2, f_3, f_4, f_5, f_6, f_7, f_8)^{T^*}$ as shown in (16):

$$\begin{cases} \frac{dz_1^*}{dt} = \Lambda_h - \frac{b\beta_h(1-\varepsilon)z_8^*}{N_h} z_1^* - \mu_h z_1^* := f_1(z^*), \\ \frac{dz_2^*}{dt} = \frac{b\beta_h(1-\varepsilon)z_8^*}{N_h} z_1^* - k_1 z_2^* := f_2(z^*), \\ \frac{dz_3^*}{dt} = k_7 z_2^* - k_2 z_3^* := f_3(z^*), \\ \frac{dz_4^*}{dt} = k_8 z_2^* - k_3 z_4^* := f_4(z^*), \\ \frac{dz_5^*}{dt} = \phi\alpha_h z_2^* + \gamma_a z_3^* + k_6 z_4^* - \mu_h z_5^* := f_5(z^*), \\ \frac{dz_6^*}{dt} = (1-\tau_2\xi)\Lambda_v - \frac{b\beta_v(1-\varepsilon)(\eta z_3^* + z_4^*)}{N_h} z_6^* - k_5 z_6^* := f_6(z^*), \\ \frac{dz_7^*}{dt} = \frac{b\beta_v(1-\varepsilon)(\eta z_3^* + z_4^*)}{N_h} z_6^* - k_4 z_7^* := f_7(z^*), \\ \frac{dz_8^*}{dt} = \alpha_v z_7^* - k_5 z_8^* := f_8(z^*), \end{cases} \tag{16}$$

and as defined before, $k_1 = \alpha_h + \mu_h$, $k_2 = \gamma_a + \mu_h$, $k_3 = \gamma_i + \tau_1\delta + \mu_h$, $k_4 = \alpha_v + \mu_v + \tau_2\xi$, $k_5 = \mu_v + \tau_2\xi$, $k_6 = \gamma_i + \tau_1\delta$, $k_7 = (1-\phi)\nu\alpha_h$, $k_8 = (1-\phi)(1-\nu)\alpha_h$. The transformed model at the DFE has a Jacobian matrix given as

$$J(\mathscr{E}_f) = \begin{pmatrix} -\mu_h & 0 & 0 & 0 & 0 & 0 & 0 & -b\beta_h(1-\varepsilon) \\ 0 & -k_1 & 0 & 0 & 0 & 0 & 0 & b\beta_h(1-\varepsilon) \\ 0 & k_7 & -k_2 & 0 & 0 & 0 & 0 & 0 \\ 0 & k_8 & 0 & -k_3 & 0 & 0 & 0 & 0 \\ 0 & \phi\alpha_h & \gamma_a & k_6 & -\mu_h & 0 & 0 & 0 \\ 0 & 0 & -\frac{b\beta_v(1-\varepsilon)^2\eta\Lambda_v\Lambda_h}{(\mu_v+\tau_2\xi)\mu_h} & -\frac{b\beta_v(1-\varepsilon)^2\Lambda_v\Lambda_h}{(\mu_v+\tau_2\xi)\mu_h} & 0 & -k_5 & 0 & 0 \\ 0 & 0 & \frac{b\beta_v(1-\varepsilon)^2\eta\Lambda_v\Lambda_h}{(\mu_v+\tau_2\xi)\mu_h} & \frac{b\beta_v(1-\varepsilon)^2\Lambda_v\Lambda_h}{(\mu_v+\tau_2\xi)\mu_h} & 0 & 0 & -k_4 & 0 \\ 0 & 0 & 0 & 0 & 0 & 0 & \alpha_h & -k_5 \end{pmatrix}.$$

Now, consider the case when $\mathscr{R}_t = 1$, we can choose β_h^* as the bifurcation parameter and solving for β_h from the expression for $\mathscr{R}_t = 1$, we have

$$\beta_h^* = \frac{k_1k_2k_3k_4k_5(\mu_v + \tau_2\xi)\Lambda_h}{(1-\varepsilon)^2b^2\beta_v(1-\phi)\alpha_h\mu_h(k_3\eta\nu + k_2(1-\nu))\alpha_v\Lambda_v(1-\xi)}. \tag{17}$$

It can be proven that the converted system (16), having $\beta_h = \beta_h^*$, does have a nonhyperbolic equilibrium point with a simple eigenvalue with zero real part and all other eigenvalues with negative real parts in the linearized system [34]. As a result, the dynamics of the model (16) near $\beta_h = \beta_h^*$ can be studied using the center manifold theory (CMT) [35].

Eigenvectors of $J(\mathscr{E}_f)|_{\beta_h=\beta_h^*}$ The right eigenvector in relation to the zero eigenvalue evaluated at $J(\mathscr{E}_f)|_{\beta_h=\beta_h^*}$ is denoted by

$$\mathbf{W} = [w_1, w_2, w_3, w_4, w_5, w_6, w_7, w_8],$$

with the components obtained as $w_1 = -\frac{b\beta_h(1-\varepsilon)}{k_5}w_8, w_2 = w_2 > 0, w_3 = \frac{k_7}{k_2}w_2, w_4 = \frac{k_8}{k_3}w_2, w_5 = \frac{\phi\alpha_h w_2 + \gamma_a w_3 + k_6 w_4}{\mu_h}, w_6 = -\frac{(Aw_3 + Bw_4)}{k_5}, w_7 = \frac{Aw_3 + Bw_4}{k_4}, w_8 = \frac{\alpha_h}{k_5}w_7$, where $A = \frac{b\beta_v(1-\varepsilon)^2\eta\Lambda_v\Lambda_h}{(\mu_v+\tau_2\xi)\mu_h}$ and $B = \frac{b\beta_v(1-\varepsilon)^2\Lambda_v\Lambda_h}{(\mu_v+\tau_2\xi)\mu_h}$. In addition, the left eigenvector, denoted as $\mathbf{V}$, in relation to the zero eigenvalue evaluated at $J(\mathscr{E}_f)|_{\beta_h=\beta_h^*}$ satisfying the property $\mathbf{W}.\mathbf{V} = 1$, is defined by

$$\mathbf{V} = [v_1, v_2, v_3, v_4, v_5, v_6, v_7, v_8],$$

with the calculated components given as $v_1 = 0, v_2 = v_2 > 0, v_3 = 0, v_4 = \frac{k_1}{k_8}v_2, v_5 = 0, v_6 = 0, v_7 = 0, v_8 = \frac{b\beta_h(1-\varepsilon)}{k_5}v_2$.

Computations of bifurcation coefficients **a** *and* **b**

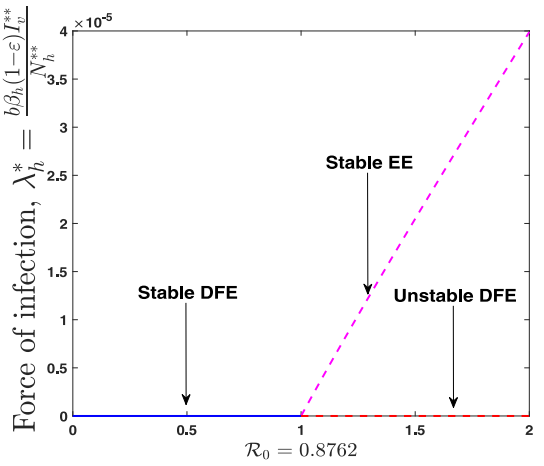

(a) Forward bifurcation.

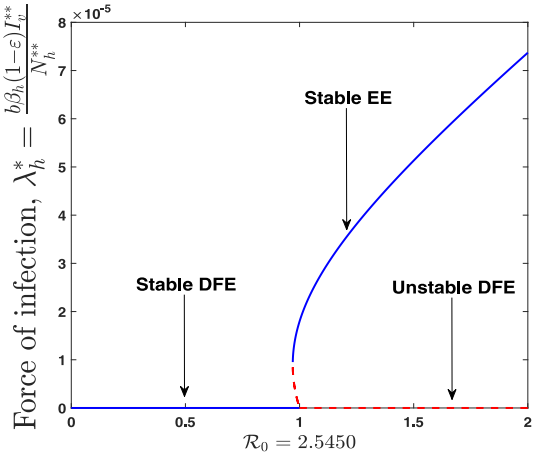

(b) Forward bifurcation.

Fig. 1. Bifurcation diagrams (a) $\beta_h = 0.2, \beta_v = 0.2$. (b) $\beta_h = 0.75, \beta_v = 0.45$, while all other parameters are fixed at the given values in Table 3.

Utilizing Castillo-Chavez and Song's notation in [35], we have

$$\mathbf{a} = \sum_{k,i,j=1}^{8} v_k w_i w_j \frac{\partial^2 f_k}{\partial z_i^* \partial z_j^*}(\mathscr{E}_f), \quad \mathbf{b} = \sum_{k,i=1}^{8} v_k w_i \frac{\partial^2 f_k}{\partial z_i^* \partial \beta_h^*}(\mathscr{E}_f). \tag{18}$$

Thus, from Eq. (18), we have the following:

$$\frac{\partial^2 f_2}{\partial z_2^* \partial z_8^*} = -\frac{b\beta_h^*(1-\varepsilon)\Lambda_h}{\mu_h}, \quad \frac{\partial^2 f_2}{\partial z_8^* \partial \beta_h^*} = b(1-\varepsilon).$$

It follows that

$$\mathbf{a} = -\frac{b\beta_h^*(1-\varepsilon)\Lambda_h}{\mu_h} v_2 w_2 w_8 < 0, \quad \mathbf{b} = v_2 w_8 b(1-\varepsilon) > 0.$$

Therefore, Theorem 4.1 of Castillo-Chavez and Song [35] indicates that the proposed model exhibits forward bifurcation at $\mathscr{R}_t = 1$. Fig. 1 shows the numerical output of the above established analysis. The ramification of the above result tells us that if the disease transmission dynamics is categorized as shown by the system (2), we can control the disease in a community that uses preventive measures. As a result of the establishment of the existence of forward bifurcation, one can proceed to show the global stabilities of the equilibrium points of the proposed model (2). □

3.2.4. Global stability of DFE, $\mathscr{E}_f$

Since DFE $\mathscr{E}_f$ is the unique equilibrium of the dengue model (2) whenever the corresponding reproduction number $\mathscr{R}_t$ is below unity, we are left to show that DFE is globally asymptotically stable (GAS). To this aim, we use the direct Lyapunov method. Suppose the positive constants $a_i > 0$ $(i = 1, 2, \ldots, 5)$ are defined as

$$a_1 = \frac{N_h^* k_4 k_5}{b\beta_h(1-\varepsilon)S_h^*}, \quad a_2 = \frac{b\beta_v(1-\varepsilon)\eta\alpha_v S_v^*}{N_h^* k_2}, \quad a_3 = \frac{b\beta_v(1-\varepsilon)\alpha_v S_v^*}{N_h^* k_3}, \quad a_4 = \alpha_v, \quad a_5 = k_4. \tag{19}$$

Then, consider the Lyapunov function $\mathscr{W} : \mathscr{D} \to \mathbb{R}$ defined as

$$\mathscr{W} = a_1 E_h + a_2 A_h + a_3 I_h + a_4 E_v + a_5 I_v. \tag{20}$$

The time derivative of $\mathscr{W}$ in Eq. (20) is

$$\begin{aligned}\frac{d\mathscr{W}}{dt} &= a_1\frac{dE_h}{dt} + a_2\frac{dA_h}{dt} + a_3\frac{dI_h}{dt} + a_4\frac{dE_v}{dt} + a_5\frac{dI_v}{dt},\\ &= \left[-a_1k_1 + a_2(1-\phi)\nu\alpha_h + a_3(1-\phi)(1-\nu)\alpha_h\right]E_h + \left[a_4\frac{b\beta_v(1-\varepsilon)\eta S_v}{N_h} - a_2k_2\right]A_h\\ &\quad + \left[a_4\frac{b\beta_v(1-\varepsilon)S_v}{N_h} - a_3k_3\right]I_h + \left(a_5\alpha_v - a_4k_4\right)E_v + \left[a_1\frac{b\beta_h(1-\varepsilon)S_h}{N_h} - a_5k_5\right]I_v.\end{aligned} \tag{21}$$

Replacing a_i $(i = 1, 2, \ldots, 5)$ in Eq. (21) by their respective terms in Eq. (19), and using the fact that $S_h \leq S_h^* = \frac{\Lambda_h}{\mu_h}$, $S_v \leq S_v^* \frac{\Lambda_v(1-\tau_2\xi)}{(\mu_v+\tau_2\xi)}$ and $N_h \leq N_h^* = S_h^*$ in $\mathscr{D}$, we obtain

$$\frac{d\mathscr{W}}{dt} \leq \left[\frac{b\beta_v(1-\varepsilon)\alpha_v\alpha_h(1-\phi)[k_3\eta\nu + k_2(1-\nu)]S_v^*}{N_h^*k_2k_3} - \frac{N_h^*k_1k_4k_5}{b\beta_h(1-\varepsilon)S_h^*}\right]E_h, \tag{22}$$

$$\frac{d\mathscr{W}}{dt} \leq \frac{k_1k_4k_5}{b\beta_h(1-\varepsilon)}\left[\frac{b^2(1-\varepsilon)^2\beta_h\beta_v\alpha_v\alpha_h(1-\phi)[k_3\eta\nu + k_2(1-\nu)]S_v^*}{k_1k_2k_3k_4k_5S_h^*} - 1\right]E_h, \tag{23}$$

$$\frac{d\mathscr{W}}{dt} \leq \frac{k_1k_4k_5}{b\beta_h(1-\varepsilon)}\left(\mathscr{R}_t^2 - 1\right)E_h. \tag{24}$$

Therefore, $\frac{d\mathscr{W}}{dt} \leq 0$ if $\mathscr{R}_t \leq 1$, with $\frac{d\mathscr{W}}{dt} = 0$ if $\mathscr{R}_t = 1$ or $E_h = 0$. Further, $A_h = 0$, $I_h = 0$, $E_v = 0$ and $I_v = 0$ whenever $E_h = 0$. Substituting $E_h = A_h = I_h = E_v = I_v = 0$ in Eqs. (2a) and (2f) yields $S_h(t) \to S_h^* = N_h^*$ and $S_v(t) \to S_v^* = N_v^*$ as $t \to \infty$. Thus,

$$[S_h(t), E_h(t), A_h(t), I_h(t), R_h(t), S_v(t), E_v(t), I_v(t)] \to \mathscr{E}_f$$

as $t \to \infty$. It follows from LaSalle's invariance principle [36] that every solution of the dengue model (2) with initial conditions in $\mathscr{D}$ converges to DFE $\mathscr{E}_f$ as $t \to \infty$. Therefore, the DFE $\mathscr{E}_f$ of the dengue model (2) is GAS in $\mathscr{D}$ expressed by Eq. (4) if $\mathscr{R}_t < 1$, since the Lyapunov function is positive and zero at the equilibria. Hence, we claim the following result.

Theorem 3.2. *If $\mathscr{R}_t \leq 1$, then the DFE $\mathscr{E}_f$ of model (2) is GAS in $\mathscr{D}$ given by (4), and it is unstable otherwise.*

The epidemiological implication of Theorem 3.2 is that dengue elimination is possible regardless of the initial sizes of the sub-populations of model (2) whenever $\mathscr{R}_t \leq 1$. This result is graphically illustrated in Fig. 2.

3.2.5. Global stability of DPE, $\mathscr{E}_p$

Suppose

$$\mathscr{D}_0 = \{(S_h(t), E_h(t), A_h(t), I_h(t), R_h(t), S_v(t), E_v(t), I_v(t)) \in \mathscr{D} : E_h(t) = A_h(t) = I_h(t) = R_h(t) = E_v(t) = I_v(t) = 0\} \tag{25}$$

is defined as the stable manifold of DFE, $\mathscr{E}_f$. Then, we summarize the result of the global asymptomatic stability of DPE $\mathscr{E}_p$ in the following result.

Theorem 3.3. *If $\mathscr{R}_t > 1$, then DPE $\mathscr{E}_p$ of model (2) is GAS in the interior of region $\mathscr{D}\backslash\mathscr{D}_0$.*

Proof. It is easy to exclude the differential Eq. (2e) describing the dynamics of the recovered human subpopulation, R_h, from the dengue model (2) as R_h is not coupled with the other state variables in the remaining differential equations. Then, following [26,37,38], we make use of the Goh–Volterra type Lyapunov function $\mathscr{Y} : \mathscr{D}\backslash\mathscr{D}_0 \to \mathbb{R}$ defined in (26) as

$$\begin{aligned}\mathscr{Y} = {} & b_1\left(S_h - S_h^{**} - S_h^{**}\ln\frac{S_h}{S_h^{**}}\right) + b_2\left(E_h - E_h^{**} - E_h^{**}\ln\frac{E_h}{E_h^{**}}\right) + b_3\left(A_h - A_h^{**} - A_h^{**}\ln\frac{A_h}{A_h^{**}}\right)\\ & + b_4\left(I_h - I_h^{**} - I_h^{**}\ln\frac{I_h}{I_h^{**}}\right) + b_5\left(S_v - S_v^{**} - S_v^{**}\ln\frac{S_v}{S_v^{**}}\right) + b_6\left(E_v - E_v^{**} - E_v^{**}\ln\frac{E_v}{E_v^{**}}\right)\\ & + b_7\left(I_v - I_v^{**} - I_v^{**}\ln\frac{I_v}{I_v^{**}}\right),\end{aligned} \tag{26}$$

with suitably determined coefficients $b_i > 0$ $(i = 1, 2, \ldots, 7)$ as

$$\begin{aligned} & b_1 = b_2 = \frac{N_h^{**}\beta_v(\eta A_h^{**} + I_h^{**})\alpha_v S_v^{**}}{N_h^{**}\beta_h I_v^{**}S_h^{**}},\ b_3 = \frac{b\beta_v(1-\varepsilon)\alpha_v\eta A_h^{**}S_v^{**}}{N_h^{**}(1-\phi)\nu\alpha_h E_h^{**}},\ b_4 = \frac{b\beta_v(1-\varepsilon)\alpha_v I_h^{**}S_v^{**}}{N_h^{**}(1-\phi)(1-\nu)\alpha_h E_h^{**}},\\ & b_5 = b_6 = \alpha_v,\ b_7 = k_4 = \frac{b\beta_v(1-\varepsilon)(\eta A_h^{**} + I_h^{**})S_v^{**}}{N_h^{**}E_h^{**}}.\end{aligned} \tag{27}$$

The time derivative of $\mathscr{Y}$ in Eq. (26) along the solutions of model (2) is given by

$$\begin{aligned}\frac{d\mathscr{Y}}{dt} = {} & b_1\left(\frac{dS_h}{dt} - \frac{S_h^{**}}{S_h}\frac{dS_h}{dt}\right) + b_2\left(\frac{dE_h}{dt} - \frac{E_h^{**}}{E_h}\frac{dE_h}{dt}\right) + b_3\left(\frac{dA_h}{dt} - \frac{A_h^{**}}{A_h}\frac{dA_h}{dt}\right) + b_4\left(\frac{dI_h}{dt} - \frac{I_h^{**}}{I_h}\frac{dI_h}{dt}\right)\\ & + b_5\left(\frac{dS_v}{dt} - \frac{S_v^{**}}{S_v}\frac{dS_v}{dt}\right) + b_6\left(\frac{dE_v}{dt} - \frac{E_v^{**}}{E_v}\frac{dE_v}{dt}\right) + b_7\left(\frac{dI_v}{dt} - \frac{I_v^{**}}{I_v}\frac{dI_v}{dt}\right).\end{aligned} \tag{28}$$

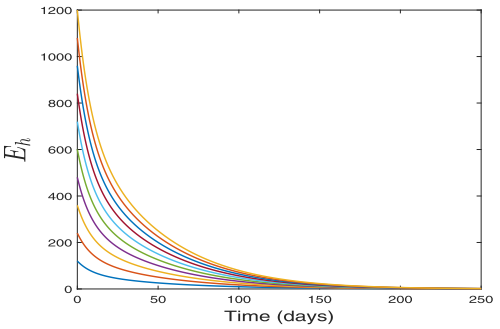

(a) Stability plot for exposed humans

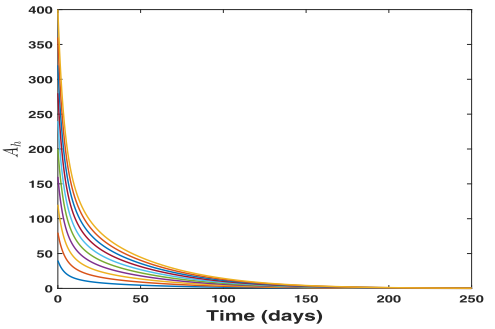

(b) Stability plot for asymptomatic humans

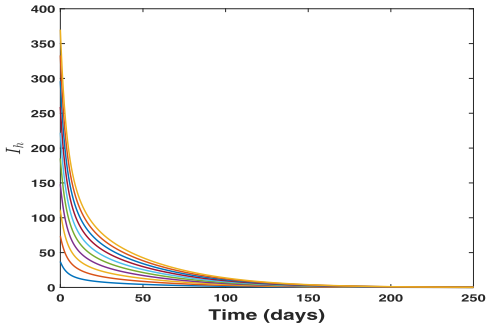

(c) Stability plot for symptomatic humans

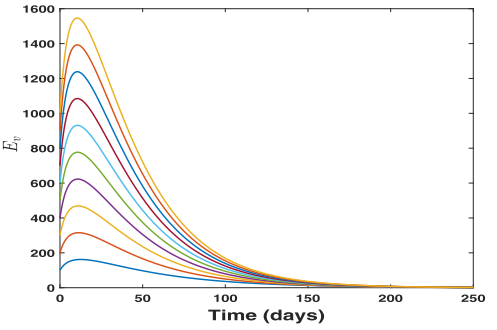

(d) Stability plot for exposed vectors

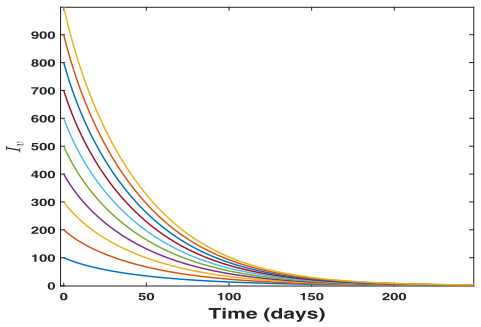

(e) Stability plot for infectious vectors

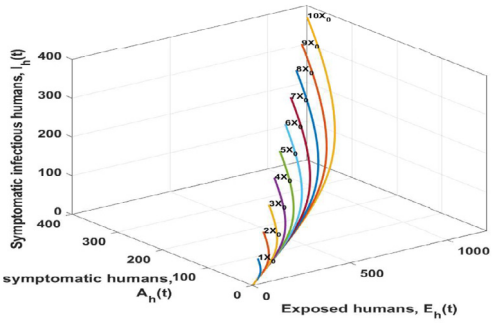

(f) 3D stability plot, $X_0 = [3247503, 120, 40, 37, 0, 12990600, 100, 100]$, X_0 is the initial conditions

Fig. 2. Global stability plots for the DFE by taking $b = 0.16272$, $\beta_h = 0.55$, $\beta_v = 0.55$, $\gamma_a = 0.028833$, $\alpha_v = 0.00396$ so that $\mathscr{R}_t = 0.3661 < 1$.

At equilibrium, the below relations in (29) hold from the dengue model (2).

$$
\begin{aligned}
\Lambda_h &= \frac{b\beta_h(1-\varepsilon)I_v^{**}S_h^{**}}{N_h^*} + \mu_h S_h^*, \quad (1-\tau_2\xi)\Lambda_v = \frac{b\beta_v(1-\varepsilon)(\eta A_h^{**} + I_h^{**})S_v^{**}}{N_h^{**}} + k_5 S_v^{**},\\
k_1 &= \frac{b\beta_h(1-\varepsilon)I_v^{**}S_h^{**}}{N_h^{**}E_h^{**}}, \qquad k_4 = \frac{b\beta_v(1-\varepsilon)(\eta A_h^{**} + I_h^{**})S_v^{**}}{N_h^{**}E_v^{**}},\\
k_2 &= \frac{(1-\phi)\nu\alpha_h E_h^{**}}{A_h^{**}}, \qquad k_5 = \frac{\alpha_v E_v^{**}}{I_v^{**}},\\
k_3 &= \frac{(1-\phi)(1-\nu)\alpha_h E_h^{**}}{I_h^{**}}, \qquad N_h = N_h^{**} = \frac{\Lambda_h}{\mu_h}.
\end{aligned}
\tag{29}
$$

So,

$$\begin{aligned}\frac{d\mathscr{Y}}{dt} &= b_1\left[\mu_h S_h^{**}\left(2-\frac{S_h}{S_h^{**}}-\frac{S_h^{**}}{S_h}\right)\right]\\ &+ b_1\left[\frac{b\beta_h(1-\varepsilon)I_v^{**}S_h^{**}}{N_h^{**}}-\frac{S_h^{**2}}{S_h}\frac{b\beta_h(1-\varepsilon)I_v^{**}}{N_h^{**}}-\frac{b\beta_h(1-\varepsilon)I_vS_hE_h^{**}}{N_h^{**}E_h}+\frac{b\beta_h(1-\varepsilon)I_v^{**}S_h^{**}}{N_h^{**}E_h^{**}}E_h^{**}\right]\\ &+ b_3\left[-(1-\phi)\nu\alpha_h\frac{E_hA_h^{**}}{A_h}+\frac{(1-\phi)\nu\alpha_hE_h^{**}}{A_h^{**}}A_h^{**}\right]\\ &+ b_4\left[-(1-\phi)(1-\nu)\alpha_h\frac{E_hI_h^{**}}{I_h}+\frac{(1-\phi)(1-\nu)\alpha_hE_h^{**}}{I_h^{**}}I_h^{**}\right]\\ &+ b_5\left[k_5S_v^{**}\left(2-\frac{S_v}{S_v^{**}}-\frac{S_v^{**}}{S_v}\right)\right]\\ &+ b_5\left[\frac{b\beta_v(1-\varepsilon)(\eta A_h^{**}+I_h^{**})S_v^{**}}{N_h^{**}}-\frac{S_v^{**2}}{S_v}\frac{b\beta_v(1-\varepsilon)(\eta A_h^{**}+I_h^{**})}{N_h^{**}}-\frac{b\beta_v(1-\varepsilon)(\eta A_h+I_h)S_vE_v^{**}}{N_h^{**}E_v}\right.\\ &\left.+\frac{b\beta_v(1-\varepsilon)(\eta A_h^{**}+I_h^{**})S_v^{**}}{N_h^{**}E_v^{**}}E_v^{**}\right]+b_7\left[-\alpha_v\frac{E_vI_v^{**}}{I_v}+\frac{\alpha_vE_v^{**}}{I_v^{**}}I_v^{**}\right].\end{aligned}\tag{30}$$

Replacing the coefficients b_i $(i=1,2\ldots,7)$ in (30) with their terms as defined in (27), and simplifying gives

$$\begin{aligned}\frac{d\mathscr{Y}}{dt} &= \frac{\beta_v(\eta A_h^{**}+I_h^{**})\alpha_v\mu_hS_v^{**}}{\beta_hI_v^{**}}\left(2-\frac{S_h}{S_h^{**}}-\frac{S_h^{**}}{S_h}\right)+5\frac{b\beta_v(1-\varepsilon)\alpha_v\eta A_h^{**}S_v^{**}}{N_h^{**}}+5\frac{b\beta_v(1-\varepsilon)\alpha_vI_h^{**}S_v^{**}}{N_h^{**}}\\ &- \frac{b\beta_v(1-\varepsilon)\alpha_v\eta A_h^{**}S_v^{**}S_h^{**}}{N_h^{**}S_h}-\frac{b\beta_v(1-\varepsilon)\alpha_vI_h^{**}S_v^{**}S_h^{**}}{N_h^{**}S_h}\\ &- \frac{b\beta_v(1-\varepsilon)\alpha_v\eta A_h^{**}E_h^{**}S_v^{**}I_vS_h}{N_h^{**}I_v^{**}S_h^{**}E_h}-\frac{b\beta_v(1-\varepsilon)\alpha_vI_h^{**}E_h^{**}S_v^{**}I_vS_h}{N_h^{**}I_v^{**}S_h^{**}E_h}\\ &- \frac{b\beta_v(1-\varepsilon)\alpha_v\eta A_h^{**}S_v^{**}}{N_h^{**}}\frac{E_hA_h^{**}}{E_h^{**}A_h}-\frac{b\beta_v(1-\varepsilon)\alpha_vI_h^{**}S_v^{**}}{N_h^{**}}\frac{E_hI_h^{**}}{E_h^{**}I_h}\\ &+ \frac{\alpha_v^2E_v^{**}S_v^{**}}{I_v^{**}}\left(2-\frac{S_v}{S_v^{**}}-\frac{S_v^{**}}{S_v}\right)-\frac{b\beta_v(1-\varepsilon)\alpha_v\eta A_h^{**}S_v^{**}}{N_h^{**}}\frac{S_v^{**}}{S_v}-\frac{b\beta_v(1-\varepsilon)\alpha_vI_h^{**}S_v^{**}}{N_h^{**}}\frac{S_v^{**}}{S_v}\\ &- \frac{b\beta_v(1-\varepsilon)\alpha_v\eta A_hS_vE_v^{**}}{N_h^{**}E_v}-\frac{b\beta_v(1-\varepsilon)\alpha_vI_hS_vE_v^{**}}{N_h^{**}E_v}\\ &+ \frac{b\beta_v(1-\varepsilon)\alpha_v\eta A_h^{**}S_v^{**}E_v^{**}}{N_h^{**}E_h^{**}}+\frac{b\beta_v(1-\varepsilon)\alpha_vI_h^{**}S_v^{**}E_v^{**}}{N_h^{**}E_h^{**}}\\ &- \frac{b\beta_v(1-\varepsilon)\alpha_v\eta A_h^{**}S_v^{**}}{N_h^{**}}\frac{E_vI_v^{**}}{E_h^{**}I_v}-\frac{b\beta_v(1-\varepsilon)\alpha_vI_h^{**}S_v^{**}}{N_h^{**}}\frac{E_vI_v^{**}}{E_h^{**}I_v}.\end{aligned}\tag{31}$$

Then,

$$\begin{aligned}\frac{d\mathscr{Y}}{dt} &= \frac{\beta_v(\eta A_h^{**}+I_h^{**})\alpha_v\mu_hS_v^{**}}{\beta_hI_v^{**}}\left(2-\frac{S_h}{S_h^{**}}-\frac{S_h^{**}}{S_h}\right)+\frac{\alpha_v^2E_v^{**}S_v^{**}}{I_v^{**}}\left(2-\frac{S_v}{S_v^{**}}-\frac{S_v^{**}}{S_v}\right)\\ &+ \frac{b\beta_v(1-\varepsilon)\alpha_v\eta A_h^{**}S_v^{**}}{N_h^{**}}\left(5-\frac{S_h^{**}}{S_h}-\frac{I_vS_hE_h^{**}}{I_v^{**}S_h^{**}E_h}-\frac{E_hA_h^{**}}{E_h^{**}A_h}-\frac{S_v^{**}}{S_v}-\frac{E_v^{**}A_hS_v}{E_vA_h^{**}S_v^{**}}\right)\\ &+ \frac{b\beta_v(1-\varepsilon)\alpha_vI_h^{**}S_v^{**}}{N_h^{**}}\left(5-\frac{S_h^{**}}{S_h}-\frac{I_vS_hE_h^{**}}{I_v^{**}S_h^{**}E_h}-\frac{E_hI_h^{**}}{E_h^{**}I_h}-\frac{S_v^{**}}{S_v}-\frac{E_v^{**}I_hS_v}{E_vI_h^{**}S_v^{**}}\right)\\ &+ \frac{b\beta_v(1-\varepsilon)\alpha_v\eta A_h^{**}S_v^{**}E_v^{**}}{N_h^{**}E_h^{**}}\left(1-\frac{E_vI_v^{**}}{E_v^{**}I_v}\right)+\frac{b\beta_v(1-\varepsilon)\alpha_vI_h^{**}S_v^{**}E_v^{**}}{N_h^{**}E_h^{**}}\left(1-\frac{E_vI_v^{**}}{E_v^{**}I_v}\right).\end{aligned}\tag{32}$$

Since arithmetic mean is greater than or equal to geometric mean, it follows that

$$\left(1-\frac{E_vI_v^{**}}{E_v^{**}I_v}\right)\le 0,\ \left(2-\frac{S_h}{S_h^{**}}-\frac{S_h^{**}}{S_h}\right)\le 0,\ \left(2-\frac{S_v}{S_v^{**}}-\frac{S_v^{**}}{S_v}\right)\le 0,$$
$$\left(5-\frac{S_h^{**}}{S_h}-\frac{I_vS_hE_h^{**}}{I_v^{**}S_h^{**}E_h}-\frac{E_hA_h^{**}}{E_h^{**}A_h}-\frac{S_v^{**}}{S_v}-\frac{E_v^{**}A_hS_v}{E_vA_h^{**}S_v^{**}}\right)\le 0,$$
$$\left(5-\frac{S_h^{**}}{S_h}-\frac{I_vS_hE_h^{**}}{I_v^{**}S_h^{**}E_h}-\frac{E_hI_h^{**}}{E_h^{**}I_h}-\frac{S_v^{**}}{S_v}-\frac{E_v^{**}I_hS_v}{E_vI_h^{**}S_v^{**}}\right)\le 0.$$

Therefore, $\frac{d\mathscr{V}}{dt} \leq 0$ since all the model parameters are positive, with $\frac{d\mathscr{V}}{dt} = 0$ if and only if $S_h = S_h^{**}$, $E_h = E_h^{**}$, $A_h = A_h^{**}$, $I_h = I_h^{**}$, $S_v = S_v^{**}$, $E_v = E_v^{**}$ and $I_v = I_v^{**}$. Hence, by LaSalle's invariance principle [36],

$$(S_h(t), E_h(t), A_h(t), I_h(t), S_v(t), E_v(t), I_v(t)) \to \left(S_h^{**}, E_h^{**}, A_h^{**}, I_h^{**}, S_v^{**}, E_v^{**}, I_v^{**}\right) \text{ as } t \to \infty. \tag{33}$$

Now, using $\limsup_{t\to\infty} E_h(t) = E_h^{**}$, $\limsup_{t\to\infty} A_h(t) = A_h^{**}$ and $\limsup_{t\to\infty} I_h(t) = I_h^{**}$ (which implied from (33)), and for sufficiently small $\epsilon > 0$, there exist three nonnegative constants C_i ($i = 1, 2, 3$) such that $\limsup_{t\to\infty} E_h(t) \leq E_h^{**} + \epsilon$ for $t > C_1$, $\limsup_{t\to\infty} A_h(t) \leq A_h^{**} + \epsilon$ for $t > C_2$ and $\limsup_{t\to\infty} I_h(t) \leq I_h^{**} + \epsilon$ for $t > C_3$. Thus, for $t > \max\{C_i\}$ (where $i = 1, 2, 3$), it follows from (2e) that

$$\frac{dR_h}{dt} \leq \phi\alpha_h(E_h^{**} + \epsilon) + \gamma_a(A_h^{**} + \epsilon) + (\gamma_i + \tau_1\delta)(I_h^{**} + \epsilon) - \mu_h R_h. \tag{34}$$

By applying comparison theorem, we obtain

$$\limsup_{t\to\infty} R_h(t) \leq \frac{\phi\alpha_h(E_h^{**} + \epsilon) + \gamma_a(A_h^{**} + \epsilon) + (\gamma_i + \tau_1\delta)(I_h^{**} + \epsilon)}{\mu_h}. \tag{35}$$

It follows from (35) that as $\epsilon \to 0$,

$$\limsup_{t\to\infty} R_h(t) \leq \frac{\phi\alpha_h E_h^{**} + \gamma_a A_h^{**} + (\gamma_i + \tau_1\delta)I_h^{**}}{\mu_h}. \tag{36}$$

Furthermore, in a similar manner, it can be shown using $\liminf_{t\to\infty} E_h(t) = E_h^{**}$, $\liminf_{t\to\infty} A_h(t) = A_h^{**}$ and $\liminf_{t\to\infty} I_h(t) = I_h^{**}$ (as implied from (33)), that

$$\liminf_{t\to\infty} R_h(t) \geq \frac{\phi\alpha_h E_h^{**} + \gamma_a A_h^{**} + (\gamma_i + \tau_1\delta)I_h^{**}}{\mu_h}. \tag{37}$$

Consequently, from (36) and (37), one gets

$$\liminf_{t\to\infty} R_h(t) \geq \frac{\phi\alpha_h E_h^{**} + \gamma_a A_h^{**} + (\gamma_i + \tau_1\delta)I_h^{**}}{\mu_h} \geq \limsup_{t\to\infty} R_h(t), \tag{38}$$

implying that

$$\lim_{t\to\infty} R_h(t) = \frac{\phi\alpha_h E_h^{**} + \gamma_a A_h^{**} + (\gamma_i + \tau_1\delta)I_h^{**}}{\mu_h} = R_h^{**}. \tag{39}$$

Combining (33) and (39) gives rise to

$$\lim_{t\to\infty} (S_h(t), E_h(t), A_h(t), I_h(t), R_h(t), S_v(t), E_v(t), I_v(t)) = \left(S_h^{**}, E_h^{**}, A_h^{**}, I_h^{**}, R_h^{**}, S_v^{**}, E_v^{**}, I_v^{**}\right) = \mathscr{E}_p.$$

Therefore, DPE $\mathscr{E}_p$ is GAS whenever $\mathscr{R}_t > 1$. □

From biological viewpoint, Theorem 3.3 implies that regardless of the initial sizes of the infectious humans in the population, dengue will establish itself in the community if $\mathscr{R}_t > 1$. This result is graphically illustrated in Fig. 3.

3.3. Sensitivity analysis

3.3.1. Local sensitivity analysis

In the sense of the approach previously used by many authors [27,37,39], analysis of the sensitivity of parameters of model (2) with respect to the dengue threshold quantity (control reproduction number, $\mathscr{R}_t$) is conducted to assess how importance the sensitive parameters are to the dynamics of the model. The epidemiological insights arising from the analysis may be helpful in developing effective control intervention strategies to curtail dengue transmission and spread.

The normalized forward-sensitivity index is defined as

$$\Lambda_{p_i^*}^{\mathscr{R}_t} = \frac{\partial\mathscr{R}_t}{\partial p_i^*} \times \frac{p_i^*}{\mathscr{R}_t}, \tag{40}$$

where, p_i^* represent the various parameters in $\mathscr{R}_t$. The close form solutions from the above equation is given as

$$\Lambda_{\Lambda_h}^{\mathscr{R}_t} = -\frac{1}{2},\ \Lambda_b^{\mathscr{R}_t} = 1,\ \Lambda_{\beta_h}^{\mathscr{R}_t} = \frac{1}{2},\ \Lambda_{\beta_v}^{\mathscr{R}_t} = \frac{1}{2},\ \Lambda_{\Lambda_v}^{\mathscr{R}_t} = \frac{1}{2},$$

$$\Lambda_{\mu_h}^{\mathscr{R}_t} = \frac{A_0^* + A_1^* + A_2^* + 2\,\alpha_h\,\delta\,\gamma_a\,\mu_h\,\nu\,\tau_1 - 2\,\alpha_h\,\delta\,\eta\,\gamma_a\,\gamma_i\,\nu\,\tau_1 - 2\,\alpha_h\,\delta\,\eta\,\gamma_a\,\mu_h\,\nu\,\tau_1}{2\,(\alpha_h + \mu_h)\,(\gamma_a + \mu_h)\,((\gamma_a + \mu_h)\,(\nu - 1) - \eta\,\nu\,(\gamma_i + \mu_h + \delta\,\tau_1))\,(\gamma_i + \mu_h + \delta\,\tau_1)},$$

$$\Lambda_{\eta}^{\mathscr{R}_t} = \frac{\Lambda_v\,\alpha_h\,\alpha_v\,b^2\,\beta_h\,\beta_v\,\eta\,\mu_h\,\nu\,(1-\phi)\,(1-\varepsilon)^2\,(1-\xi)}{\Lambda_h\,(\mu_v + \tau_2\,\xi)^2\,(\alpha_h + \mu_h)\,(\gamma_a + \mu_h)\,(\alpha_v + \mu_v + \tau_2\,\xi)\,2A_3^*},$$

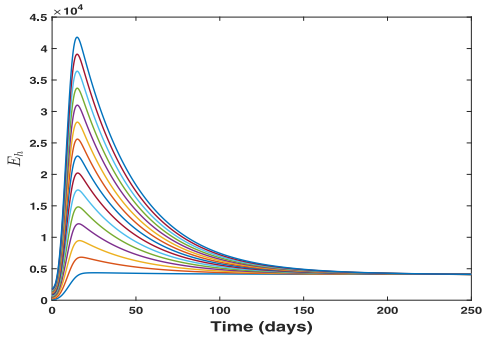

(a) Stability plot for exposed humans

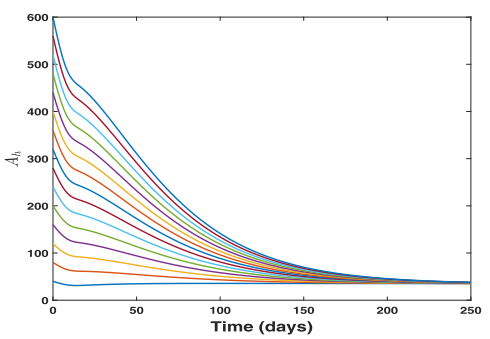

(b) Stability plot for asymptomatic humans

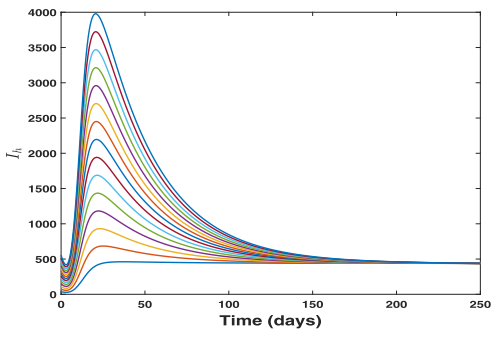

(c) Stability plot for symptomatic humans

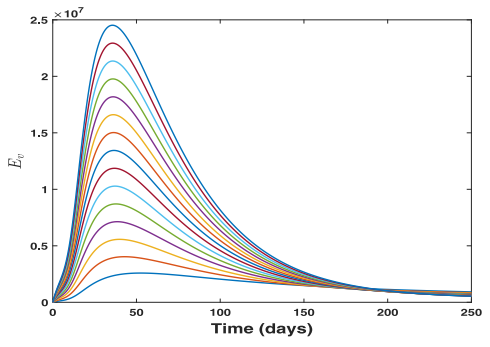

(d) Stability plot for exposed vectors

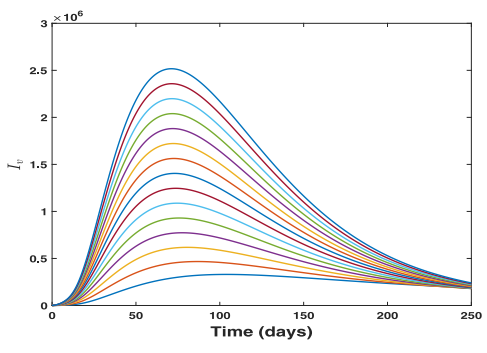

(e) Stability plot for infected vectors

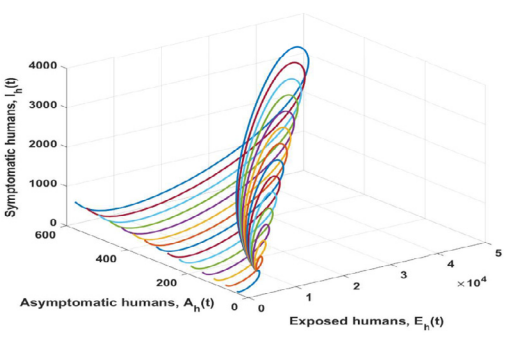

(f) 3D stability plot, $X_0 = [3240, 120, 40, 37, 0, 12990600, 100, 100]$

Fig. 3. Global stability plots for the DPE using $b = 0.4272, \beta_h = 0.45, \beta_v = 0.45, \gamma_a = 0.028833, \gamma_i = 0.228833, \alpha_h = 0.02899, \eta = 0.4000, \alpha_v = 0.00396, \mu_v = 0.0238, \nu = 0.01000, \varepsilon = 0.01, \phi = 0.15, \delta = 0.05, \xi = 0.01, \tau_1 = 0.002$ and $\tau_2 = 0.01$ so that $\mathscr{R}_t = 1.5538 > 1$.

$$\Lambda_{\alpha_v}^{\mathscr{R}_t} = \frac{\mu_v + \tau_2\,\xi}{2\,(\alpha_v + \mu_v + \tau_2\,\xi)},\ \Lambda_{\mu_v}^{\mathscr{R}_t} = -\frac{\mu_v\,(2\,\alpha_v + 3\,\mu_v + 3\,\tau_2\,\xi)}{2\,(\mu_v + \tau_2\,\xi)\,(\alpha_v + \mu_v + \tau_2\,\xi)},$$

$$\Lambda_{\nu}^{\mathscr{R}_t} = -\frac{\nu\,(\eta\,\gamma_i - \mu_h - \gamma_a + \eta\,\mu_h + \delta\,\eta\,\tau_1)}{2\,((\gamma_a + \mu_h)\,(\nu - 1) - \eta\,\nu\,(\gamma_i + \mu_h + \delta\,\tau_1))},$$

$$\Lambda_{\gamma_a}^{\mathscr{R}_t} = -\frac{\eta\,\gamma_a\,\nu\,(\gamma_i + \mu_h + \delta\,\tau_1)}{2\,(\gamma_a + \mu_h)\,((\gamma_a + \mu_h)\,(1 - \nu) + \eta\,\nu\,(\gamma_i + \mu_h + \delta\,\tau_1))},$$

$$\Lambda_{\gamma_i}^{\mathscr{R}_t} = -\frac{\gamma_i\,(\gamma_a + \mu_h)\,(1 - \nu)}{2\,((\gamma_a + \mu_h)\,(1 - \nu) + \eta\,\nu\,(\gamma_i + \mu_h + \delta\,\tau_1))\,(\gamma_i + \mu_h + \delta\,\tau_1)},$$

$$\Lambda_{\alpha_h}^{\mathscr{R}_t} = \frac{\mu_h}{2\,(\alpha_h + \mu_h)},\ \Lambda_{\varepsilon}^{\mathscr{R}_t} = -\frac{\varepsilon}{(1 - \varepsilon)},\ \Lambda_{\phi}^{\mathscr{R}_t} = -\frac{\phi}{2\,(1 - \phi)},\ \Lambda_{\tau_2}^{\mathscr{R}_t} = -\frac{\tau_2\,\xi\,(2\,\alpha_v + 3\,\mu_v + 3\,\tau_2\,\xi)}{2\,(\mu_v + \tau_2\,\xi)\,(\alpha_v + \mu_v + \tau_2\,\xi)},$$

Table 2
Normalized Forward-Sensitivity Indexes in relation to Table 3 .

Parameter	Value	Parameter	Value
b	1.000	Λ_h	−0.5000
β_h	0.5000	μ_v	−1.1151
Λ_v	0.5000	γ_a	−0.1927
η	0.1928	ϕ	−0.0882
β_v	0.5000	ν	−0.1145
μ_h	0.5000	γ_i	−0.2938
α_h	1.4347×10^{-4}	ε	−0.0101
α_v	0.4430	τ_1	−0.0134
τ_2	−0.3280	δ	−0.0134
ξ	−0.3330		

$$\Lambda_{\delta}^{\mathscr{R}_t} = -\frac{\delta\,\tau_1\,(\gamma_a+\mu_h)\,(1-\nu)}{2\,((\gamma_a+\mu_h)\,(1-\nu)+\eta\,\nu\,(\gamma_i+\mu_h+\delta\,\tau_1))\,(\gamma_i+\mu_h+\delta\,\tau_1)},$$
$$\Lambda_{\xi}^{\mathscr{R}_t} = -\frac{A_4^*\xi\left(\mu_v{}^2-\mu_v\,\tau_2\,\xi+3\,\mu_v\,\tau_2+\alpha_v\,\mu_v-2\,\tau_2{}^2\,\xi^2+3\,\tau_2{}^2\,\xi-\alpha_v\,\tau_2\,\xi+2\,\alpha_v\,\tau_2\right)}{2\,(\mu_v+\tau_2\,\xi)\,((\gamma_a+\mu_h)\,(1-\nu)+\eta\,\nu\,(\gamma_i+\mu_h+\delta\,\tau_1))\,(1-\xi)\,(\alpha_v+\mu_v+\tau_2\,\xi)},$$
$$\Lambda_{\tau_1}^{\mathscr{R}_t} = -\frac{\delta\,\tau_1\,(\gamma_a+\mu_h)\,(1-\nu)}{2\,((\gamma_a+\mu_h)\,(1-\nu)+\eta\,\nu\,(\gamma_i+\mu_h+\delta\,\tau_1))\,(\gamma_i+\mu_h+\delta\,\tau_1)},$$

where,

$$A_0^{**} = \alpha_h\,\gamma_a{}^2\,\gamma_i\,\nu-\alpha_h\,\delta\,\gamma_a{}^2\,\tau_1+\alpha_h\,\gamma_i\,\mu_h{}^2\,\nu-\alpha_h\,\delta\,\mu_h{}^2\,\tau_1+2\,\eta\,\gamma_i\,\mu_h{}^3\,\nu,$$
$$A_0^{*} = 2\,\gamma_a\,\mu_h{}^3-\mu_h{}^4\,\nu+\mu_h{}^4+\gamma_a{}^2\,\mu_h{}^2+\eta\,\mu_h{}^4\,\nu-2\,\gamma_a\,\mu_h{}^3\,\nu-\gamma_a{}^2\,\mu_h{}^2\,\nu-\alpha_h\,\gamma_a{}^2\,\gamma_i-\alpha_h\,\gamma_i\,\mu_h{}^2+A_0^{**},$$
$$A_1^{**} = -2\,\alpha_h\,\delta\,\gamma_a\,\mu_h\,\tau_1+\delta^2\,\eta\,\mu_h{}^2\,\nu\,\tau_1{}^2-\alpha_h\,\eta\,\gamma_a\,\gamma_i{}^2\,\nu-\alpha_h\,\eta\,\gamma_a\,\mu_h{}^2\,\nu+\alpha_h\,\delta\,\gamma_a{}^2\,\nu\,\tau_1,$$
$$A_1^{*} = \eta\,\gamma_i{}^2\,\mu_h{}^2\,\nu-2\,\alpha_h\,\gamma_a\,\gamma_i\,\mu_h+2\,\alpha_h\,\gamma_a\,\gamma_i\,\mu_h\,\nu+A_1^{**},$$
$$A_2^{*} = \alpha_h\,\delta\,\mu_h{}^2\,\nu\,\tau_1+2\,\delta\,\eta\,\mu_h{}^3\,\nu\,\tau_1+2\,\delta\,\eta\,\gamma_i\,\mu_h{}^2\,\nu\,\tau_1-\alpha_h\,\delta^2\,\eta\,\gamma_a\,\nu\,\tau_1{}^2-2\,\alpha_h\,\eta\,\gamma_a\,\gamma_i\,\mu_h\,\nu,$$
$$A_3^{*} = \frac{\Lambda_v\,\alpha_h\,\alpha_v\,b^2\,\beta_h\,\beta_v\,\mu_h\,((\gamma_a+\mu_h)\,(1-\nu)+\eta\,\nu\,(\gamma_i+\mu_h+\delta\,\tau_1))\,(1-\phi)\,(1-\varepsilon)^2\,(1-\xi)}{\Lambda_h\,(\mu_v+\tau_2\,\xi)^2\,(\alpha_h+\mu_h)\,(\gamma_a+\mu_h)\,(\gamma_i+\mu_h+\delta\,\tau_1)\,(\alpha_v+\mu_v+\tau_2\,\xi)},$$
$$A_4^{*} = (\gamma_a+\mu_h-\gamma_a\,\nu-\mu_h\,\nu+\eta\,\gamma_i\,\nu+\eta\,\mu_h\,\nu+\delta\,\eta\,\nu\,\tau_1)\,.$$

Now, using the parameter values in Table 3, Table 2 shows the numerical values of the above analytic results. The epidemiological insight from Table 2 is that a 0.5 reduction in Λ_h will have a corresponding reduction in the spread of dengue, b increased by 1 will lead to 1% increase in the basic reproduction number, β_h, β_v, Λ_v and μ_h equal to 0.5 means that an increase in any of the parameters will lead to 0.5 increase in the spread of dengue. This idea holds for the other numerical values in Table 2. Therefore, Table 2 indicates that the most sensitive parameter in the proposed model is the mosquito biting rate, b.

3.3.2. Latin hypercube sampling

Here, we investigate the global sensitivities of the model parameters using scatter plots and the Latin hypercube sampling (LHS). Scatter plots are sometimes used to visually examine the connection between the basic reproduction number and model parameters, or between model output variables and parameters [39,40]. More sensitive parameters give an evident association, with a clear correlation pattern in the scatter plot [39,40]. LHS is a Monte Carlo sampling technique. It divides the range of each parameter into n even intervals and takes one sample from each interval randomly just once [39,40]. LHS is often used in conjunction with the partial rank correlation coefficient (PRCC) to quantify the nonlinear, but unmodulated, link between parameters or variables [39,40]. We utilize a sample size of $n = 1000$ to determine the dependency of parameters in the control reproduction number. The scatter plots are displayed in supplementary information. The partial rank correction coefficients (PRCC) values of the parameters are shown in Fig. 4(a). The longer bars in Fig. 4(a) indicate that those factors have a significant statistical impact on the control reproduction number, $\mathscr{R}_t$. On the other hand, the uncertainty analysis (UA) in Fig. 4(b) shows that the range of $\mathscr{R}_t$ is approximately $[1-4]$, though most of the outputs are concentrated in low values ($[1-2.6]$).

4. Dengue model with optimal control and its qualitative analysis

In a previous study [4], model (2) was used to analyse the impact of personal protection using insecticide-treated bed nets (ITNs) or mosquito-repellent lotion (ε), treatment drug therapy for latently infected individuals (ϕ), chemotherapy or treatment of symptomatic infectious individuals (δ) and effort of mosquito reduction with application of open space spray of insecticide (ξ) control interventions with constant rates. Here, these four control interventions are modelled as time-dependent control functions by considering ε, ϕ, δ and ξ as $u_P(t)$, $u_E(t)$, $u_I(t)$ and $u_A(t)$, respectively.

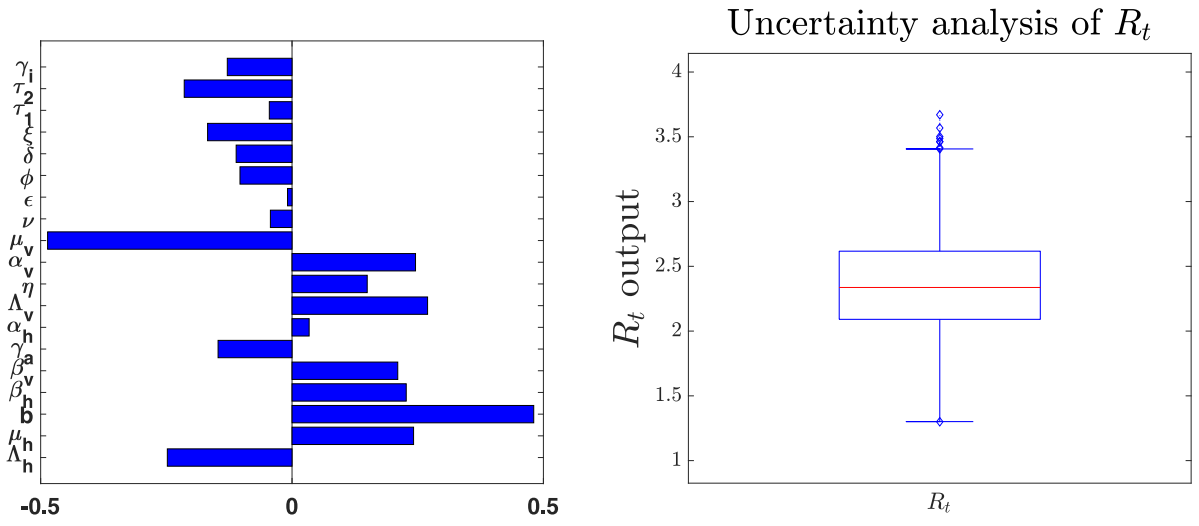

(a) Partial rank correlation coefficients (PRCC) (b) The box plot of $\mathscr{R}_t$.

Fig. 4. Global sensitivity and uncertainty analysis of $\mathscr{R}_t$.

Consequently, the autonomous system (2) is modified to form the non-autonomous system involving eight mutually exclusive time-dependent ODEs given as

$$\begin{aligned}
\frac{dS_h(t)}{dt} &= \Lambda_h - \frac{b\beta_h(1-u_P(t))I_v}{N_h}S_h - \mu_h S_h,\\
\frac{dE_h(t)}{dt} &= \frac{b\beta_h(1-u_P(t))I_v}{N_h}S_h - (\alpha_h+\mu_h)E_h,\\
\frac{dA_h(t)}{dt} &= (1-u_E(t))\nu\alpha_h E_h - (\gamma_a+\mu_h)A_h,\\
\frac{dI_h(t)}{dt} &= (1-u_E(t))(1-\nu)\alpha_h E_h - (\gamma_i+\tau_1 u_I(t)+\mu_h)I_h,\\
\frac{dR_h(t)}{dt} &= u_E(t)\alpha_h E_h + \gamma_a A_h + (\gamma_i+\tau_1 u_I(t))I_h - \mu_h R_h,\\
\frac{dS_v(t)}{dt} &= (1-\tau_2 u_A(t))\Lambda_v - \frac{b\beta_v(1-u_P(t))(\eta A_h+I_h)}{N_h}S_v - (\mu_v+\tau_2 u_A(t))S_v,\\
\frac{dE_v(t)}{dt} &= \frac{b\beta_v(1-u_P(t))(\eta A_h+I_h)}{N_h}S_v - (\alpha_v+\mu_v+\tau_2 u_A(t))E_v,\\
\frac{dI_v(t)}{dt} &= \alpha_v E_v - (\mu_v+\tau_2 u_A(t))I_v.
\end{aligned} \tag{41}$$

To reduce dengue infection burden in the community by minimizing the exposed human, asymptomatic infected human, symptomatic infectious human, exposed mosquito and infectious mosquito subpopulations and the costs associated with prevention and control measures, we make use of the cost or objective functional designed as

$$\begin{aligned}
\mathcal{J}(u_A(t),u_E(t),u_I(t),u_P(t)) = \int_0^T &[A_1E_h(t)+A_2A_h(t)+A_3I_h(t)+A_4(S_v(t)+E_v(t)+I_v(t))\\
&+B_1u_P^2(t)+B_2u_E^2(t)+B_3u_I^2(t)+B_4u_A^2(t)\big]\,dt,
\end{aligned} \tag{42}$$

where A_i and B_i $(i=1,\ldots,4)$ are the positive weight constants and T represents the final time such that $0\le t\le T$. The terms $B_1u_P^2$, $B_2u_E^2$, $B_3u_I^2$ and $B_4u_A^2$ are the respective costs associated with the use of ITNs, treatment drug therapy for latently infected humans, chemotherapy or treatment of symptomatic infectious humans and open space spray of insecticide. We consider quadratic control costs in respect of the standards in literature on optimal control problems [10,26,37,41–44]. Our interest, in particular, is to seek an optimal control quadruple $u^*=(u_i^*)$ such that

$$\mathcal{J}(u^*)=\min\left\{\mathcal{J}(u_i):u_i\in\mathscr{U}\right\}, \tag{43}$$

where $\mathscr{U}$ is a bounded Lebesgue measurable non-empty control set presented as

$$\mathscr{U} = \{u_i(t) : 0 \leq u_i(t) \leq 1,\ t \in [0, T]\}, \tag{44}$$

for $i = (P, E, I, A)$.

4.1. Qualitative analysis of optimal control problem

4.1.1. Existence of optimal controls

This section explores the existence of optimal control quadruple for optimizing (minimizing) the objective functional $\mathscr{J}$ in (42). To this aim, the existence result (see Theorem 4.1, pp. 68–69) by Fleming and Rishel [45] is employed.

Theorem 4.1. *There exists an optimal control quadruple $u^* = (u_i^*)$, with $i = (P, E, I, A)$, that minimizes the objective functional $\mathscr{J}$ in (42) constrained by the state equations in (41) over the control set $\mathscr{U}$ provided that the five properties below hold:*

(i) The optimal control set and the state variables set are not empty.
(ii) Control set $\mathscr{U}$ is closed and convex.
(iii) The right-hand side of the state system (41) is continuous and bounded by a linear functional in both the state and control variables.
(iv) The integrand of the objective functional $\mathscr{J}$ in (42) is convex over the control set $\mathscr{U}$.
(v) There exist constants $d_1, d_2 > 0$ and $d_3 > 1$ such that the integrand of the objective functional $\mathscr{J}$ in (42) is bounded below by

$$d_1 \left(|u_P|^2 + |u_E|^2 + |u_I|^2 + |u_A|^2\right)^{\frac{d_3}{2}} - d_2.$$

Proof. To prove Theorem 4.1, we verify each of the five properties as follows:

(i) The first property is satisfied, since system (41) has bounded coefficients and its solution trajectories are confined in a compact region in a finite time horizon.
(ii) The closure and convexity of the control set $\mathscr{U}$ follow immediately from the definition.
(iii) By *priori* boundedness of the state solutions, the right-hand sides of system (41) satisfy the third property.
(iv) Clearly, the integrand of the objective functional $\mathscr{J}$, denoted as $\mathscr{N}(t, x, u)$, is convex on the control set $\mathscr{U}$. Thus, we have proven the fourth property.
(v) Given the integrand $\mathscr{N}(t, x, u)$. Then,

$$\begin{aligned}\mathscr{N}(t, x, u) &= A_1E_h + A_2A_h + A_3I_h + A_4(S_v + E_v + I_v) + B_1u_P^2 + B_2u_E^2 + B_3u_I^2 + B_4u_A^2\\ &\geq B_1u_P^2 + B_2u_E^2 + B_3u_I^2 + B_4u_A^2\\ &\geq d_1 \left(|u_P|^2 + |u_E|^2 + |u_I|^2 + |u_A|^2\right)^{\frac{d_3}{2}} - d_2,\end{aligned}$$

where $d_1 = \min\{B_1, B_2, B_3, B_4\}$, $d_2 > 0$ and $d_3 = 2$. □

4.1.2. Characterization of the optimal control

Pontryagin's maximum principle [32] provides the necessary conditions that an optimal control quadruple $u^* = (u_P^*, u_E^*, u_I^*, u_A^*)$ of the dengue model (2) must satisfy. The principle helps in converting the non-autonomous system (2) together with the objective functional (42) into a problem of minimizing pointwise a Hamiltonian $\mathscr{H}$, with respect to the time-dependent controls $u_P(t)$, $u_E(t)$, $u_I(t)$ and $u_A(t)$. Associated with system (2) is the Hamiltonian obtained as

$$\mathscr{H} = \mathscr{N}(t, x, u) + \sum_j \lambda_j f_j, \tag{45}$$

where $\mathscr{N}$ is the integrand of the Lagrangian form of the objective functional $\mathscr{J}$ in (42), λ_j is the adjoint (co-state) variable and f_j is the right-hand side of the non-autonomous system (2) for $j = S_h, E_h, A_h.I_h, R_h, S_v, E_v, I_v$. To obtain the necessary conditions for the optimal control, we claim the characterization result summarized in Theorem 4.2.

Theorem 4.2. *If $u^* = (u_i^*)$, where $i = (P, E, I, A)$, is an optimal control quadruple that minimizes the objective functional $\mathscr{J}$ in (42) over the control set $\mathscr{U}$ constrained by the state system (2), then there exist co-state variables λ_{S_h}, λ_{E_h}, λ_{A_h}, λ_{I_h}, λ_{R_h}, λ_{S_v},*

λ_{E_v}, λ_{I_v} *satisfying*

$$\begin{aligned}
\frac{d\lambda_{S_h}}{dt} &= \lambda_{S_h}\mu_h + (\lambda_{S_h} - \lambda_{E_h})\frac{b\beta_h(1-u_P)I_v}{N_h} + (\lambda_{E_h} - \lambda_{S_h})\frac{b\beta_h(1-u_P)I_vS_h}{N_h^2},\\
\frac{d\lambda_{E_h}}{dt} &= -A_1 + \lambda_{E_h}(\alpha_h + \mu_h) - \left\{\left[\lambda_{A_h}\nu + \lambda_{I_h}(1-\nu)\right](1-u_E) + \lambda_{R_h}u_E\right\}\alpha_h,\\
\frac{d\lambda_{A_h}}{dt} &= -A_2 + \lambda_{A_h}(\gamma_a + \mu_h) - \lambda_{R_h}\gamma_a + (\lambda_{S_v} - \lambda_{E_v})\frac{b\beta_v(1-u_P)\eta S_v}{N_h}\\
&\quad + (\lambda_{E_v} - \lambda_{S_v})\frac{b\beta_v(1-u_P)\eta A_hS_v}{N_h^2},\\
\frac{d\lambda_{I_h}}{dt} &= -A_3 + \lambda_{I_h}(\gamma_i + \tau_1u_I + \mu_h) - \lambda_{R_h}(\gamma_i + \tau_1u_I) + (\lambda_{S_v} - \lambda_{E_v})\frac{b\beta_v(1-u_P)S_v}{N_h}\\
&\quad + (\lambda_{E_v} - \lambda_{S_v})\frac{b\beta_v(1-u_P)I_hS_v}{N_h^2},\\
\frac{d\lambda_{R_h}}{dt} &= \lambda_{R_h}\mu_h,\\
\frac{d\lambda_{S_v}}{dt} &= -A_4 + \lambda_{S_v}(\mu_v + \tau_2u_A) + (\lambda_{S_v} - \lambda_{E_v})\frac{b\beta_v(1-u_P)(\eta A_h + I_h)}{N_h},\\
\frac{d\lambda_{E_v}}{dt} &= -A_4 + \lambda_{E_v}(\alpha_v + \mu_v + \tau_2u_A) - \lambda_{I_v}\alpha_v,\\
\frac{d\lambda_{I_v}}{dt} &= -A_4 + (\lambda_{S_h} - \lambda_{E_h})\frac{b\beta_h(1-u_P)S_h}{N_h} + \lambda_{I_v}(\mu_v + \tau_2u_A),
\end{aligned} \tag{46}$$

with terminal (or boundary) conditions

$$\begin{aligned}
&\lambda_{S_h}(T) = 0,\ \lambda_{E_h}(T) = 0,\ \lambda_{A_h}(T) = 0,\ \lambda_{I_h}(T) = 0,\ \lambda_{R_h}(t) = 0,\ \lambda_{S_v}(T) = 0,\ \lambda_{E_v}(T) = 0,\\
&\lambda_{I_v}(T) = 0,
\end{aligned} \tag{47}$$

and the control characterizations

$$\begin{aligned}
u_P^* &= \min\left\{\max\left\{0, \frac{(\lambda_{E_h} - \lambda_{S_h})b\beta_hI_vS_h + (\lambda_{E_v} - \lambda_{S_v})b\beta_v(\eta A_h + I_h)S_v}{2B_1N_h}\right\}, 1\right\},\\
u_E^* &= \min\left\{\max\left\{0, \frac{\left[(\lambda_{A_h} - \lambda_{I_h})\nu + (\lambda_{I_h} - \lambda_{R_h})\right]\alpha_hE_h}{2B_2}\right\}, 1\right\},\\
u_I^* &= \min\left\{\max\left\{0, \frac{(\lambda_{I_h} - \lambda_{R_h})\tau_1I_h}{2B_3}\right\}, 1\right\},\\
u_A^* &= \min\left\{\max\left\{0, \frac{\left[\lambda_{S_v}(\Lambda_v + S_v) + \lambda_{E_v}E_v + \lambda_{I_v}I_v\right]\tau_2}{2B_4}\right\}, 1\right\}.
\end{aligned} \tag{48}$$

Proof. We first write the Hamiltonian $\mathscr{H}$ in (45) explicitly as

$$\begin{aligned}
\mathscr{H} &= A_1E_h + A_2A_h + A_3I_h + A_4N_v(S_v, E_v, I_v) + B_1u_P^2 + B_2u_E^2 + B_3u_I^2 + B_4u_A^2\\
&\quad + \lambda_{S_h}\left[\Lambda_h - \frac{b\beta_h(1-u_P(t))I_v}{N_h}S_h - \mu_hS_h\right]\\
&\quad + \lambda_{E_h}\left[\frac{b\beta_h(1-u_P(t))I_v}{N_h}S_h - (\alpha_h + \mu_h)E_h\right]\\
&\quad + \lambda_{A_h}\left[(1-u_E(t))\nu\alpha_hE_h - (\gamma_a + \mu_h)A_h\right]\\
&\quad + \lambda_{I_h}\left[(1-u_E(t))(1-\nu)\alpha_hE_h - (\gamma_i + \tau_1u_I(t) + \mu_h)I_h\right]\\
&\quad + \lambda_{R_h}\left[u_E(t)\alpha_hE_h + \gamma_aA_h + (\gamma_i + \tau_1u_I(t))I_h - \mu_hR_h\right]\\
&\quad + \lambda_{S_v}\left[(1-\tau_2u_A(t))\Lambda_v - \frac{b\beta_v(1-u_P(t))(\eta A_h + I_h)}{N_h}S_v - (\mu_v + \tau_2u_A(t))S_v\right]\\
&\quad + \lambda_{E_v}\left[\frac{b\beta_v(1-u_P(t))(\eta A_h + I_h)}{N_h}S_v - (\alpha_v + \mu_v + \tau_2u_A(t))E_v\right]\\
&\quad + \lambda_{I_v}\left[\alpha_vE_v - (\mu_v + \tau_2u_A(t))I_v\right].
\end{aligned} \tag{49}$$

Table 3
Parameter values used in simulating model (2).

Parameter	Value	Source	Parameter	Value	Source
Λ_h	120.2407	[4]	μ_h	$\frac{1}{74\times365}$	[4,46]
b	0.66272	[4,10]	β_h	0.75	[4,16]
β_v	0.75	[4,16]	γ_a	0.328833	[4,16]
γ_i	0.328833	[4,16]	α_h	0.12899	[4,10]
Λ_v	231978.5714	[4]	η	0.6000	[4]
α_v	0.00396	[4,10]	μ_v	$\frac{1}{42}$	[4,10]
ν	0.5000	[4]	ε	0.01	Assumed
ϕ	0.15	Assumed	δ	0.05	Assumed
ξ	0.01	Assumed	τ_1	0.3	[4]
τ_2	0.7	[4]			

Then, the co-state system (46) is determined from

$$-\frac{d\lambda_j}{dt} = \frac{\partial \mathscr{H}}{\partial j}, \tag{50}$$

where $j = S_h, E_h, A_h, I_h, R_h, S_v, E_v, I_v$ with terminal conditions (47). In addition, the optimal control quadruple $u^* = (u_P^*, u_E^*, u_I^*, u_A^*)$ given by (48) follows from the direct solution of the partial differential equations:

$$\frac{\partial \mathscr{H}}{\partial u_i} = 0 \text{ for } u_i^*, \tag{51}$$

where $i = P, E, I, A$. By standard control arguments, the use of bounds on the controls leads to the characterization

$$u_i^* = \begin{cases} 0 & \text{if } \psi_i^* \le 0 \\ \psi_i^* & \text{if } 0 \le \psi_i^* \le 1 \\ 1 & \text{if } \psi_i^* \ge 1 \end{cases} \tag{52}$$

for $i = \{P, E, I, A\}$ and where

$$\psi_P^* = \frac{(\lambda_{E_h} - \lambda_{S_h})b\beta_h I_v S_h + (\lambda_{E_v} - \lambda_{S_v})b\beta_v(\eta A_h + I_h)S_v}{2B_1 N_h},$$
$$\psi_E^* = \frac{\left[(\lambda_{A_h} - \lambda_{I_h})\nu + (\lambda_{I_h} - \lambda_{R_h})\right]\alpha_h E_h}{2B_2},$$
$$\psi_I^* = \frac{(\lambda_{I_h} - \lambda_{R_h})\tau_1 I_h}{2B_3},$$
$$\psi_A^* = \frac{\left[\lambda_{S_v}(\Lambda_v + S_v) + \lambda_{E_v}E_v + \lambda_{I_v}I_v\right]\tau_2}{2B_4}. \quad \square$$

5. Numerical simulations and cost-effectiveness analysis

To numerically demonstrate the impact of using five different combinations of the four control parameters consider in the dengue model (2) on the transmission of dengue in interacting human and mosquito populations, most of the model parameter values are taken from a previous study [4], and are as reproduced in Table 3, with ICs $S_h(0) = 3247503$, $E_h(0) = 120$, $A_h(0) = 40$, $I_h(0) = 37$, $R_h(0) = 0$, $S_v(0) = 12990600$, $E_v(0) = 100$ and $I_v(0) = 100$ [4].

5.1. Numerical simulations of the non-autonomous model

To find the optimal control strategies to minimize dengue fever spread at minimum costs, the 16-dimensional optimality system is solved numerically by an iterative method of fourth-order Runge–Kutta forward–backward sweep method implemented in MATLAB. The two-point boundary value problem optimality system consists of the state Eq. (41) coupled with the costate Eqs. (46) with ICs at time $t = 0$, the terminal conditions given in (47) and the optimal control characterization in (48). The optimality system has different time orientation, and as a result, the state Eqs. (41) with ICs at $t = 0$ and the controls initial guess are solved forward in time over the simulated time. Using the solutions of the current iteration, the costate system (46) is solved backward in time owing to the terminal conditions expressed in (47). For details of the numerical procedure, see Lenhart and Workman [47].

The impacts of different combinations of any three of the four optimal control intervention strategies are demonstrated on the dynamics of dengue fever transmission in a population by taking, in addition to the parameter values given in Table 3, the weight constants values as $A_i = 0.1$ (for $i = 1, 2, 3, 4$), $B_1 = 35$, $B_2 = 15$, $B_3 = 15$ and $B_4 = 25$. The simulations are carried out over the time interval $t \in [0, 250]$ in days.

5.1.1. Strategy A: Optimal use of ITNs, treatment drug therapy of latently infected individuals, chemotherapy or treatment of infectious individuals and open space spraying of insecticide

This control intervention strategy combines human protective effort using ITNs, $u_P(t)$ with the efforts of treatment drug therapy control for latently exposed individuals, $u_E(t)$, treatment control for symptomatic infectious individuals, $u_I(t)$, and vector control using adulticide, $u_A(t)$, to optimize the objective functional $\mathscr{J}$ given in (42). Fig. 5 shows the effect of applying this control intervention strategy on the dynamics of dengue population. It is seen that the implementation of this control strategy diminishes the sub-populations of exposed, asymptomatic and symptomatic humans, as well as the exposed and infectious mosquito sub-populations (see Figs. 5(a) to 5(e)). To minimize the objective functional $\mathscr{J}$ given in (42) optimally, Fig. 5(f) shows that control $u_P(t)$ should be held consistently at the lower bound (0%), except between the 180th and 225th days when the control needs to be held at the upper bound (100%), both controls $u_E(t)$ and $u_I(t)$ need to be increased from lower bound to about 0.19 (19%) from 210 to 225 days and remain at the lower bound throughout the remaining control intervention period, whereas the optimal control $u_A(t)$ should be held at 100% maximum level throughout the entire simulation period.

5.1.2. Strategy B: Optimal use of ITNs, treatment drug therapy of latently infected individuals and chemotherapy or treatment of infectious individuals

The prevention of humans (using ITNs) control $u_P(t)$, treatment drug therapy control of latently exposed humans, $u_E(t)$, and treatment control of symptomatic infectious humans, $u_I(t)$, are used simultaneously to optimize the objective functional $\mathscr{J}$ in (42) while we set control $u_A(t)$ to zero. Graphical illustrations of the implementation of this control intervention strategy is presented in Fig. 6. It is observed from Figs. 6(a) to 6(d) that due to this control strategy, the numbers of asymptomatic infected, exposed and symptomatic humans, and the exposed mosquitoes only reduced during the last 5 days of the control intervention period, whereas the control strategy has no significant effect on the sub-population of the symptomatic infected mosquito subpopulation as Fig. 6(e) shows. To minimize the objective functional $\mathscr{J}$ given in (42) optimally, controls $u_P(t)$ and $u_E(t)$ should be implemented at maximum coverage level (100%) during the last 10 days and kept at minimum coverage (0%) during the other times of control implementation period, while the control $u_I(t)$ is at the lower bound during the intervention period except for the need to hold it maximally from 240th day to 246th day before decreasing sharply to the lower bound at the final time of control implementation as shown in Fig. 6(f).

5.1.3. Strategy C: Optimal use of [itns], treatment drug therapy of latently infected individuals and open space spraying of insecticide

In this control intervention strategy, human protective effort using ITNs, $u_P(t)$, is combined with treatment drug therapy control of latently exposed humans, $u_E(t)$, and vector control using adulticide $u_A(t)$ to optimize the objective functional $\mathscr{J}$ in (42) while we set control $u_I(t)$ to zero. Graphical illustrations of the implementation of this control intervention strategy is shown in Fig. 7. We observe in Figs. 7(a) to 7(e) that due to the implementation of this control strategy, the sizes of exposed, asymptomatic infected and symptomatic infected humans, and exposed and symptomatic infected mosquitoes sub-populations diminish during the entire control implementation period. Fig. 7(f) depicts that to minimize the objective functional $\mathscr{J}$ given in (42) optimally, control $u_P(t)$ should be held consistently at the lower bound (0%), except between 180 and 225 days (counting from the commencement of control intervention programme) when the control needs to be implemented at maximum coverage level (100%), control $u_E(t)$ needs to be increased from lower bound (0%) to about 0.19 (19%) from 210 to 225 days and remain at the lower bound throughout the remaining control intervention period, while the optimal control $u_A(t)$ should be held at 100% maximum level throughout the period of control intervention programme.

5.1.4. Strategy D: Optimal use of ITNs, chemotherapy or treatment of infectious individuals and open space spraying of insecticide

This control intervention strategy considers the application of human protective effort using ITNs, $u_P(t)$, treatment drug therapy control of symptomatic infectious humans, $u_I(t)$, and vector control using adulticide $u_A(t)$ to optimize the objective functional $\mathscr{J}$ in (42) while we set control u_E to zero. Fig. 8 presents the dynamics of dengue population using this intervention strategy. Due to the implementation of this control strategy, the sizes of exposed, asymptomatic infected and symptomatic infected humans, and exposed and symptomatic infected mosquitoes sub-populations diminish during the entire period of control implementation period as Figs. 8(a) to 8(e) show. In Fig. 8(f), it is revealed that control $u_P(t)$ should be held maximally between 180 and 225 days (counting from the commencement of control intervention programme) while it should be sustained at the lower bound (0%) during the remaining period of control intervention, control $u_I(t)$ needs to be increased from lower bound (0%) to about 0.19 (19%) coverage between 210 and 225 days (counting from the beginning of control implementation period) and keeps at the lower bound throughout the remaining period of control intervention, whereas the optimal control $u_A(t)$ needs to be implemented at 100% maximum coverage level throughout the entire period of control intervention programme in order to minimize the objective functional $\mathscr{J}$ given in (42) optimally.

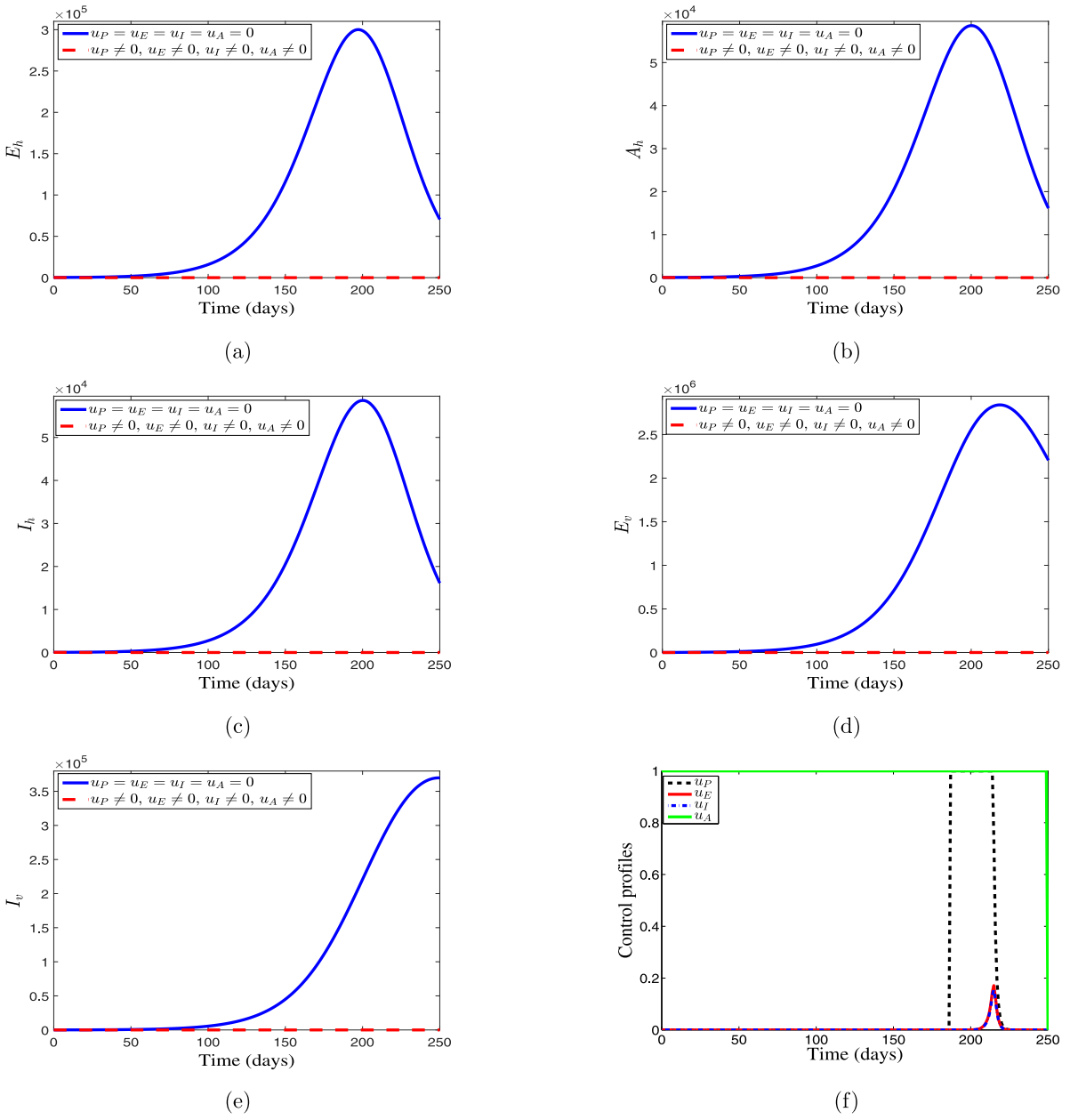

Fig. 5. Effect of Strategy A on the optimal control dengue model (41).

5.1.5. Strategy E: Optimal use of treatment drug therapy of latently infected individuals, chemotherapy or treatment of infectious individuals and open space spraying of insecticide

Here, treatment drug therapy control of latently infected humans, $u_E(t)$, treatment control of infectious individuals, $u_I(t)$, and vector control using adulticide, $u_A(t)$, are applied simultaneously to optimize the objective functional $\mathscr{J}$ in (42) while we set control $u_P(t)$ to zero. Dengue population dynamics in the interacting human and mosquito populations and optimal control profiles are demonstrated in Fig. 9. It is observed from Figs. 9(a) to 9(e) that due to the implementation of this control strategy, the sizes of exposed, asymptomatic infected and symptomatic infected humans sub-populations, as well as the exposed and symptomatic infected mosquitoes sub-populations diminish from the commencement till the end of control implementation period. In order to minimize the objective functional $\mathscr{J}$ given in (42) optimally, it is revealed in Fig. 9(f) that optimal control $u_E(t)$ only needs to be implemented at maximum level of coverage (100%) for about 46 days (between 180th and 225th days) and sustained at the lower bound for the remaining control implementation period, optimal control $u_I(t)$ should be held maximally between 165 and 225 days (counting from the commencement of

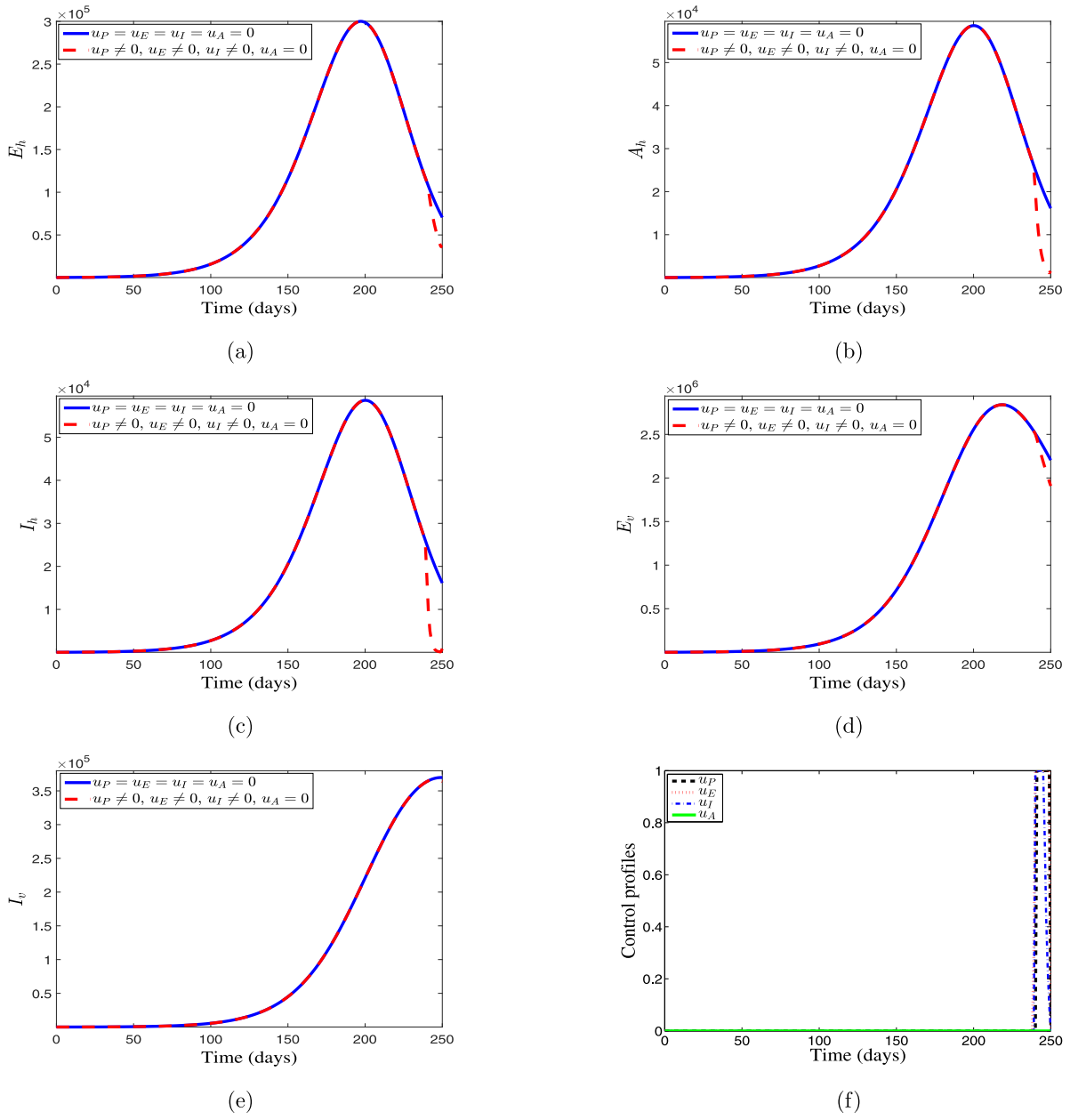

Fig. 6. Effect of Strategy B on the optimal control dengue model (41).

control intervention programme) and sustained minimally at the other times of control implementation period, whereas the optimal control $u_A(t)$ needs to be implemented at 100% maximum coverage level throughout the entire period of control intervention programme.

5.2. Cost-effectiveness analysis

By following the approach used in previous studies [9,10,37,41,43,48], the incremental cost-effectiveness ratio (ICER) is worked out to determine the least costly and most effective strategy of all the different combinations of optimal controls investigated in this paper. This cost analysis approach is concerned with the comparison of changes between the costs and health benefits associated with any two alternative control strategies competing for the same limited resources. In a

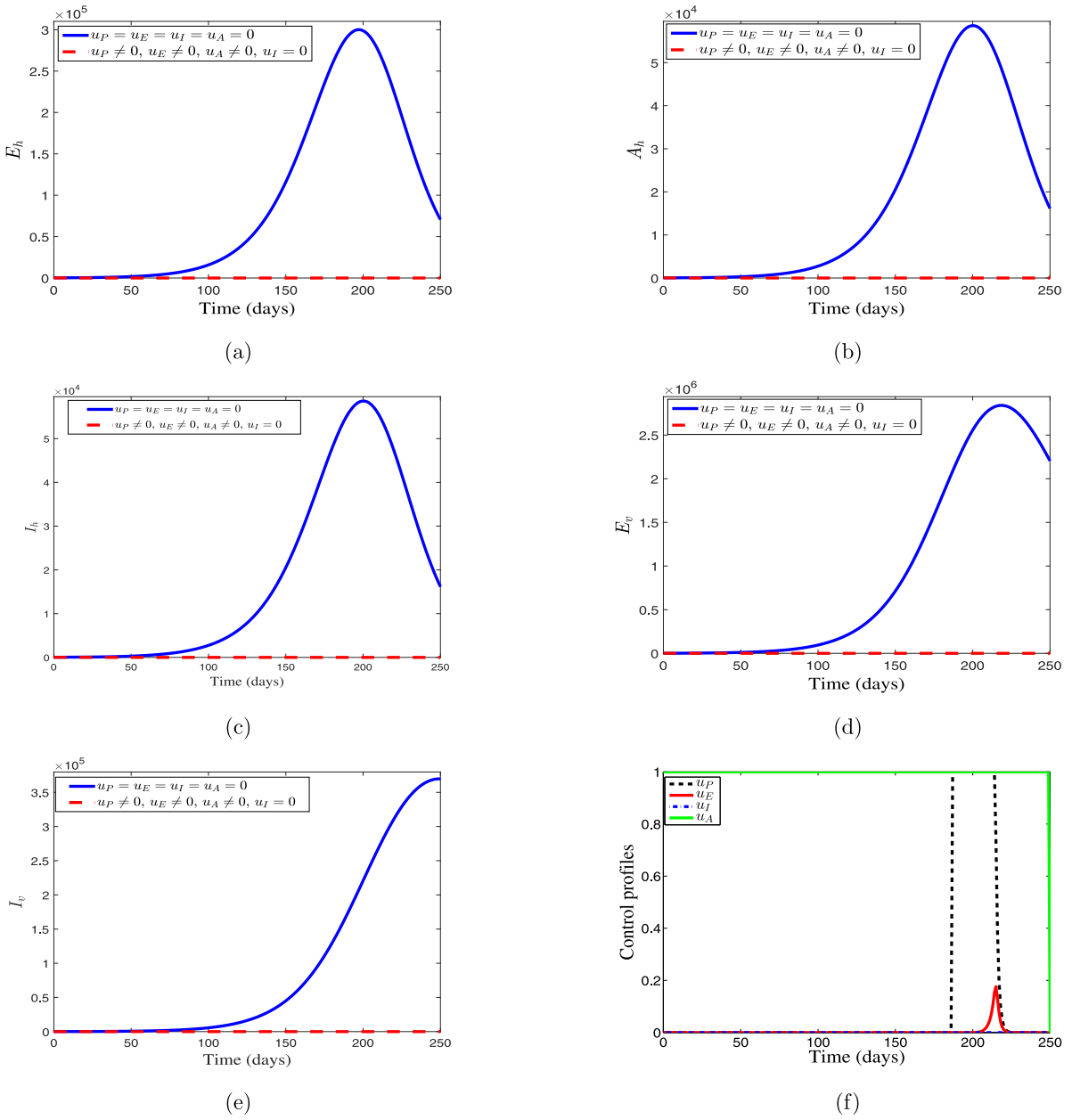

Fig. 7. Effect of Strategy C on the optimal control dengue model (41).

simple definition, ICER is given as

$$\text{ICER} = \frac{\triangle \text{ in total cost}}{\triangle \text{ in control benefits}}. \tag{53}$$

Based on the results arising from simulations of the optimality system, the control intervention strategies A, B, C, D and E are ranked from the least to the highest total number of infection averted as Table 4 shows. Thus, the ICER as shown in Table 3 is calculated for the competing intervention Strategies B and D using (53) as follows:

$$\text{ICER(B/NS)} = \frac{5.6866 \times 10^2}{2.4051 \times 10^6} = 2.3644 \times 10^{-4},$$

$$\text{ICER(B/D)} = \frac{7.2575 \times 10^3 - 5.6866 \times 10^2}{2.8840 \times 10^8 - 2.4051 \times 10^6} = 2.3388 \times 10^{-5}.$$

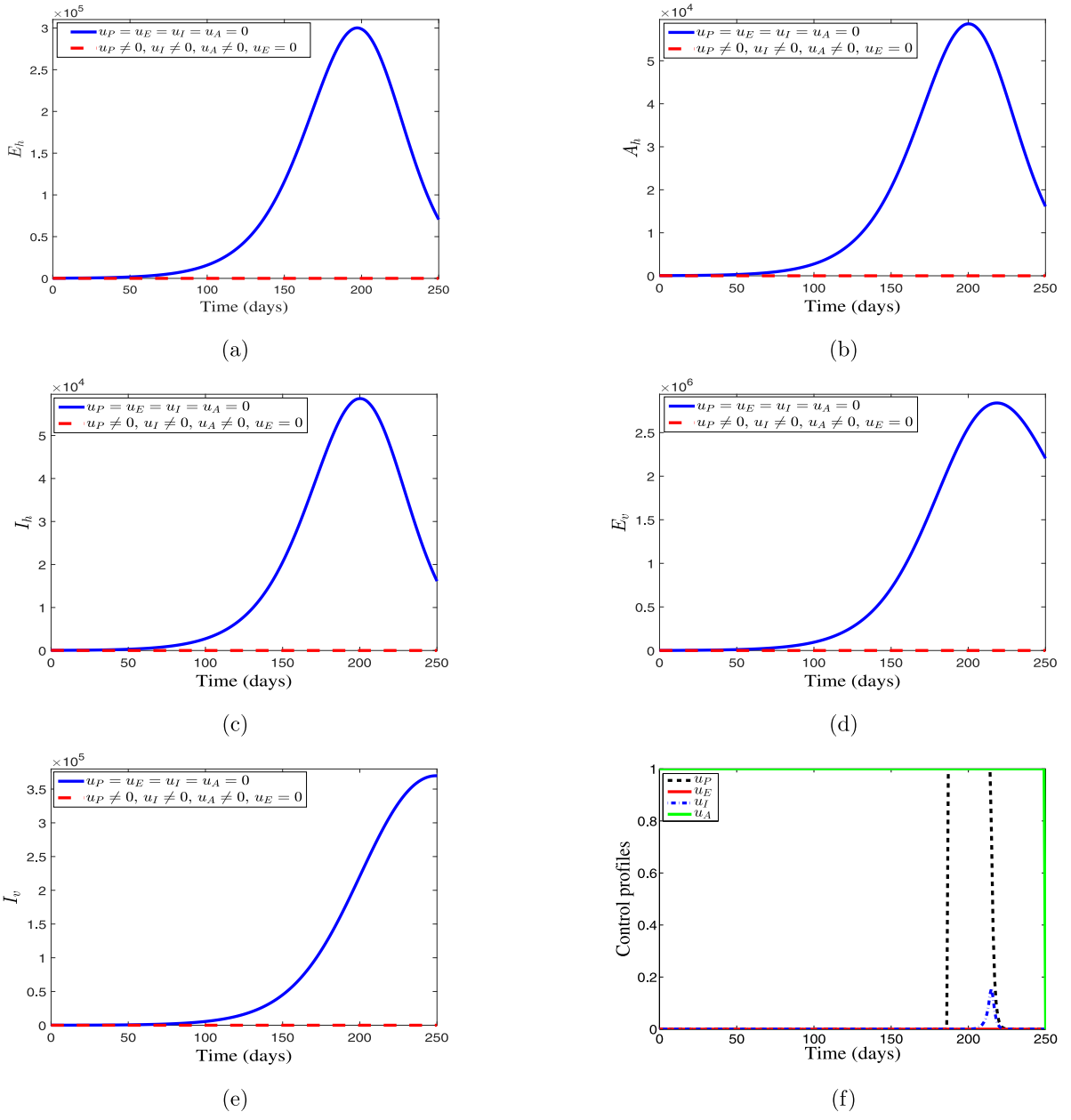

Fig. 8. Effect of Strategy D on the optimal control dengue model (41).

Table 4
Ranking of strategies A–E from least to the highest according to the infections averted .

Intervention strategy	Total infections averted	Total cost ($)	ICER
No strategy (NS)	0	0	–
B: $u_P(t), u_E(t), u_I(t)$	2.4051×10^6	5.6866×10^2	2.3644×10^{-4}
D: $u_P(t), u_I(t), u_A(t)$	2.8840×10^8	7.2575×10^3	2.3388×10^{-5}
C: $u_P(t), u_E(t), u_A(t)$	2.8840×10^8	7.2578×10^3	–
A: $u_P(t), u_E(t), u_I(t), u_A(t)$	2.8840×10^8	7.2588×10^3	–
E: $u_E(t), u_I(t), u_A(t)$	2.8840×10^8	7.4534×10^3	–

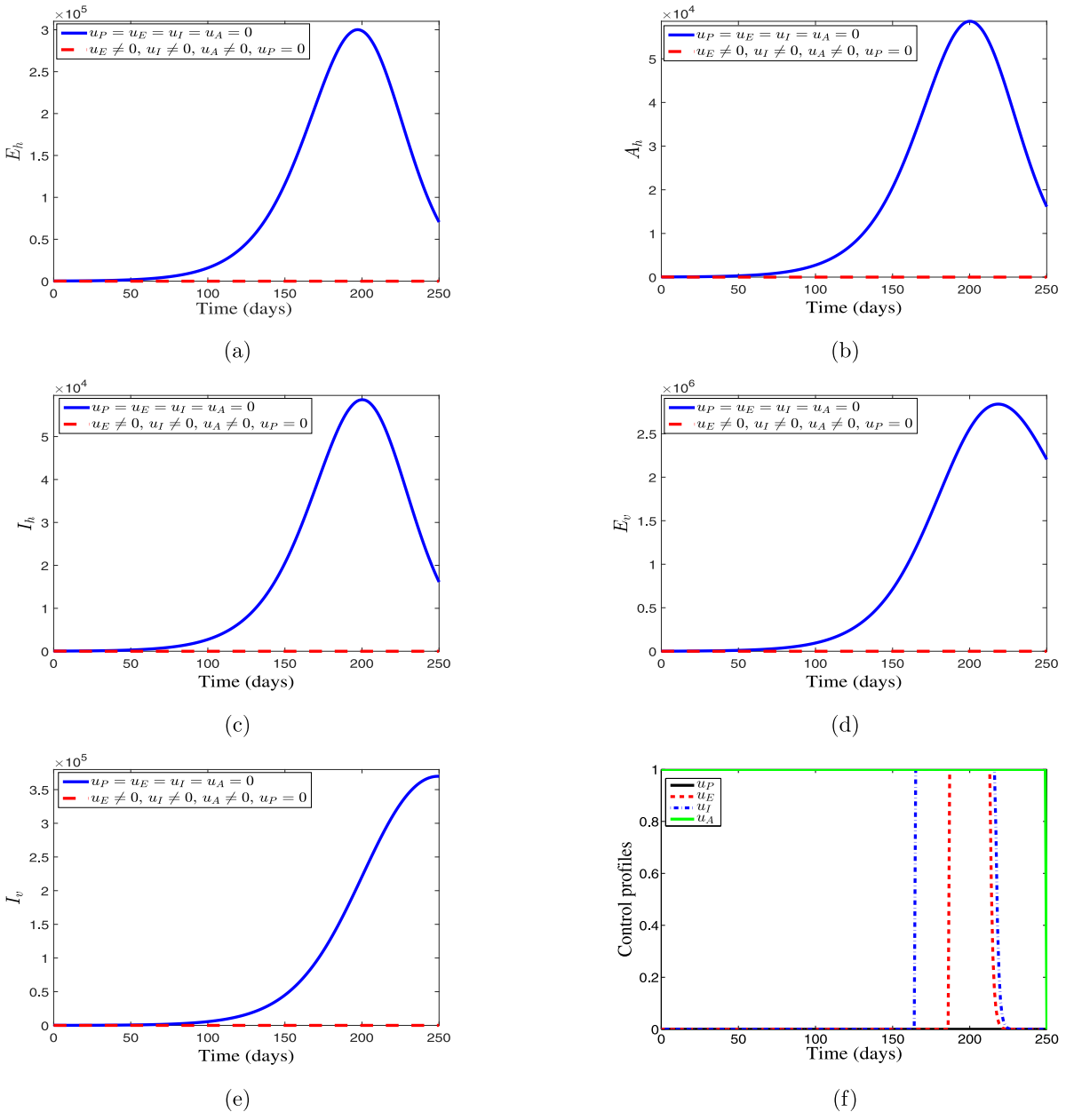

Fig. 9. Effect of Strategy E on the optimal control dengue model (41).

From Table 4, comparison of ICER(B) and ICER(D) reveals that ICER(D) is lower than ICER(B). This implies that Strategy D strongly dominates Strategy B. This simply means that Strategy D is cheaper and more effective than Strategy B. On this note, Strategy B is left out of the set of control strategies and alternative interventions to implement in order to preserve the limited available resources. At this juncture, there is no need for further re-calculation of ICER since it can be seen from Table 4 that the remaining intervention strategies (Strategy A, Strategy C, Strategy D and Strategy E) avert the same total number of infections. However, comparison of the four control intervention strategies in terms of the total cost of control implementation suggests that Strategy D requires least cost, followed by Strategy C, Strategy A, and lastly Strategy E. Consequently, control intervention Strategy D (combined efforts of optimal ITNs, chemotherapy or treatment of symptomatic infected individuals, and insecticide) is considered the most cost-effective among the five optimal control combination strategies investigated in this study. The next most cost-effective strategy is Strategy C (combination of optimal ITNs with the efforts of optimal treatment drug therapy of latently infected individuals, and insecticide), followed by Strategy A (combination of optimal ITNs, treatment drug therapy of latently infected individuals, chemotherapy or

treatment of symptomatic infected individuals, and insecticide) and Strategy E (combined effort of optimal treatment drug therapy of latently infected individuals, chemotherapy or treatment of symptomatic infected individuals, and insecticide). While the least cost-effective control intervention is Strategy B (combination of optimal ITNs, treatment drug therapy of latently infected individuals, and chemotherapy or treatment of symptomatic infected individuals).

6. Conclusion

In this paper, we studied the Lyapunov stability, bifurcation, local and global sensitivity analysis of a previously proposed non-optimal control dengue model in [4]. From the LaSalle's invariance principle, it is noticed that every solution of the dengue model converges to DFE $\mathscr{E}_f$ as $t \to \infty$. The public health explanation is that dengue elimination is possible regardless of the initial sizes of the sub-populations if the tackling of the disease follows the dynamics governed by the model. Furthermore, it is proven that DPE is globally asymptomatically stable. From a biological viewpoint, it implies that regardless of the initial size of the infectious humans in the population, dengue will establish itself in the community if and only if the threshold quantity $\mathscr{R}_t$ called "control reproduction number" is greater than unity. Based on the prior results, the local and global sensitivity analyses are studied. We then noticed that a 50% reduction in Λ_h will have a corresponding reduction in the spread of dengue, b increased by 100% will lead to 100% increase in the control reproduction number, the sensitivity indices of β_h, β_v, Λ_v and μ_h equal to 0.5 means that an increase in any of the parameters by 50% will lead to 50% increase in the spread of dengue. Therefore, these indicate that the most sensitive parameter in the proposed model is the mosquito biting rate, b, which corresponds to the scatter plot and the partial rank correlation coefficient (PRCC). Furthermore, the constant control parameters ε, ϕ, δ and ξ (representing personal protection using insecticide-treated bed nets (ITNs) or mosquito-repellent lotion, treatment drug therapy for latently infected individuals, chemotherapy or treatment of symptomatic infectious individuals, and the effort of mosquito reduction with the application of open space spray of insecticide, respectively) appearing in the non-optimal control model are considered as time-dependent control variables by extending the model to an optimal control dengue model using the concepts of optimal control theory. We establish the existence and characterization of the optimal control quadruple for the dengue model. Simulations of the effects of different strategies involving the combination of at least three of the optimal controls show the dynamical behaviours of the optimal control model. It is observed that all the strategies that include insecticide control with the use of adulticide are sufficient to optimally eliminate dengue in the population. Thus, this result highlights the significance of considering mosquito reduction through the use of insecticide (adulticide) in dengue control policy. After a careful study of the optimal control problem and simulations, we introduce cost-effectiveness analysis, which indicates that a control intervention strategy (Strategy D), which combines optimal ITNs, chemotherapy or treatment of symptomatic infected individuals and insecticide, is the most cost-effective among the five different intervention strategies considered in this paper. In the future, the discussion of feedback control can be used. Thus, the controlled variable is measured and compared to a target value.

Declaration of competing interest

The authors declare that they have no known competing financial interests or personal relationships that could have appeared to influence the work reported in this paper.

Availability of data and materials

Not applicable.

Acknowledgements

The authors are grateful to the handling editor and the anonymous reviewers for their constructive comments and suggestions that led to the presentation of this improved manuscript.

Appendix A. Supplementary data

Supplementary material related to this article can be found online at https://doi.org/10.1016/j.physa.2022.127646.

References

[1] A. Brito da Cruz, H.S. Rodrigues, Economic burden of personal protective strategies for dengue disease: an optimal control approach, in: A.I. Pereira, F.P. Fernandes, J.P. Coelho, J.P. Teixeira, M.F. Pacheco, P. Alves, R.P. Lopes (Eds.), International Conference on Optimization, Learning Algorithms and Applications, Springer, 2021, pp. 319–335.

[2] R. Rasli, Y.L. Cheong, M.K. Che Ibrahim, S.F. Farahininajua Fikri, R.N. Norzali, N.A. Nazarudin, N.F. Hamdan, K.A. Muhamed, A.A. Hafisool, R.A. Azmi, et al., Insecticide resistance in dengue vectors from hotspots in Selangor, Malaysia, PLoS Negl. Trop. Dis. 15 (3) (2021) e0009205.

[3] T. Tamura, J. Zhang, V. Madan, A. Biswas, M.P. Schwoerer, T.R. Cafiero, B.L. Heller, W. Wang, A. Ploss, Generation and characterization of genetically and antigenically diverse infectious clones of dengue virus serotypes 1-4, Emerg. Microbes Infect. (just-accepted) (2021) 1–43.

[4] A. Abidemi, H.O. Fatoyinbo, J.K.K. Asamoah, Analysis of dengue fever transmission dynamics with multiple controls: A mathematical approach, in: 2020 International Conference on Decision Aid Sciences and Application, DASA, IEEE, 2020, pp. 971–978.
[5] A. Sulekan, J. Suhaila, N.A.A. Wahid, Assessing the effect of climate factors on dengue incidence via a generalized linear model, Open J. Appl. Sci. 10 (04) (2021) 549.
[6] N. Sharma, R. Singh, C. Cattani, R. Pathak, Modeling and complexity in dynamics of T-cells and cytokines in dengue fever based on antiviral treatment, Chaos Solitons Fractals 153 (2021) 111448.
[7] L. Xue, H. Zhang, W. Sun, C. Scoglio, Transmission dynamics of multi-strain dengue virus with cross-immunity, Appl. Math. Comput. 392 (2021) 125742.
[8] World Health Organization, Managing Regional Public Goods for Health: Community-Based Dengue Vector Control, WHO Regional Office for the Western Pacific, Manila, 2013.
[9] J.K.K. Asamoah, E. Yankson, E. Okyere, G.-Q. Sun, Z. Jin, R. Jan, Optimal control and cost-effectiveness analysis for dengue fever model with asymptomatic and partial immune individuals, Results Phys. 31 (2021) 104919.
[10] A. Abidemi, N.A.B. Aziz, Optimal control strategies for dengue fever spread in Johor, Malaysia, Comput. Methods Programs Biomed. 196 (2020) 105585.
[11] C. Edussuriya, S. Deegalla, I. Gawarammana, An accurate mathematical model predicting number of dengue cases in tropics, PLoS Negl. Trop. Dis. 15 (11) (2021) e0009756.
[12] G. Knerer, C.S.M. Currie, S.C. Brailsford, Reducing dengue fever cases at the lowest budget: a constrained optimization approach applied to Thailand, BMC Public Health 21 (1) (2021) 1–14.
[13] A. Chamnan, P. Pongsumpun, I. Tang, N. Wongvanich, Local and global stability analysis of dengue disease with vaccination and optimal control, Symmetry 13 (10) (2021) 1917.
[14] A.A. Suwantika, W. Supadmi, M. Ali, R. Abdulah, Cost-effectiveness and budget impact analyses of dengue vaccination in Indonesia, PLoS Negl. Trop. Dis. 15 (8) (2021) e0009664.
[15] M.A. Khan, S.W. Shah, S. Ullah, J.F. Gómez-Aguilar, A dynamical model of asymptomatic carrier zika virus with optimal control strategies, Nonlinear Anal. RWA 50 (2019) 144–170.
[16] R. Jan, M.A. Khan, J. Gómez-Aguilar, Asymptomatic carriers in transmission dynamics of dengue with control interventions, Optim. Control Appl. Methods 41 (2) (2020) 430–447.
[17] A. Ali, Q. Iqbal, J.K.K. Asamoah, S. Islam, Mathematical modeling for the transmission potential of Zika virus with optimal control strategies, Eur. Phys. J. Plus 137 (1) (2022) 1–30.
[18] J.K.K. Asamoah, Fractal-fractional model and numerical scheme based on Newton polynomial for Q fever disease under Atangana–Baleanu derivative, Results Phys. (2022) 105189.
[19] S. Ullah, M.A. Khan, J. Gómez-Aguilar, Mathematical formulation of hepatitis B virus with optimal control analysis, Optim. Control Appl. Methods 40 (3) (2019) 529–544.
[20] E. Bonyah, M.A. Khan, K.O. Okosun, J.F. Gómez-Aguilar, On the co-infection of dengue fever and Zika virus, Optim. Control Appl. Methods 40 (3) (2019) 394–421.
[21] E. Bonyah, M.A. Khan, K.O. Okosun, J.F. Gómez-Aguilar, Modelling the effects of heavy alcohol consumption on the transmission dynamics of gonorrhea with optimal control, Math. Biosci. 309 (2019) 1–11.
[22] A. Abidemi, M.I. Abd Aziz, R. Ahmad, The impact of vaccination, individual protection, treatment and vector controls on dengue, Eng. Lett. 27 (3) (2019) 613–622.
[23] C.Q. Mentuda, Optimal control of a dengue-dengvaxia model: Csomparison between vaccination and vector control, Comput. Math. Biophys. 9 (1) (2021) 198–212.
[24] D. Aldila, Optimal control for dengue eradication program under the media awareness effect, Int. J. Nonlinear Sci. Numer. Simul. (2021) http://dx.doi.org/10.1515/ijnsns-2020-0142.
[25] A.K. Srivastav, A. Kumar, P.K. Srivastava, M. Ghosh, Modeling and optimal control of dengue disease with screening and information, Eur. Phys. J. Plus 136 (11) (2021) 1187.
[26] A. Abidemi, R. Ahmad, N.A.B. Aziz, Global stability and optimal control of dengue with two coexisting virus serotypes, MATEMATIKA: Malays. J. Ind. Appl. Math. 35 (4) (2019) 149–170.
[27] A. Abidemi, M. Abd Aziz, R. Ahmad, Vaccination and vector control effect on dengue virus transmission dynamics: Modelling and simulation, Chaos Solitons Fractals 133 (2020) 109648.
[28] A.M.C. Brito da Cruz, H.S. Rodrigues, Personal protective strategies for dengue disease: Simulations in two coexisting virus serotypes scenarios, Math. Comput. Simulation 188 (2021) 254–267.
[29] A. Abidemi, R. Ahmad, N.A.B. Aziz, Assessing the roles of human movement and vector vertical transmission on dengue fever spread and control in connected patches: from modelling to simulation, Eur. Phys. J. Plus 136 (11) (2021) 1–32.
[30] J.E. Kim, Y. Choi, J.S. Kim, S. Lee, C.H. Lee, A two-patch mathematical model for temperature-dependent dengue transmission dynamics, Processes 8 (7) (2020) 781.
[31] A. Abidemi, M.I.A. Aziz, R. Ahmad, Mathematical modelling of coexistence of two dengue virus serotypes with seasonality effect, J. Comput. Theor. Nanosci. 17 (2–3) (2020) 783–794.
[32] L.S. Pontryagin, V.G. Boltyanskii, R.V. Gamkrelidze, E.F. Mishchenko, The Mathematical Theory of Optimal Processes, Interscience, New York, 1962.
[33] P. van den Driessche, J. Watmough, Reproduction numbers and sub-threshold endemic equilibria for compartmental models of disease transmission, Math. Biosci. 180 (1) (2002) 29–48.
[34] A. B. Gumel, J. M.-S. Lubuma, O. Sharomi, Y.A. Terefe, Mathematics of a sex-structured model for syphilis transmission dynamics, Math. Methods Appl. Sci. 41 (18) (2018) 8488–8513.
[35] C. Castillo-Chavez, B. Song, Dynamical models of tuberculosis and their applications, Math. Biosci. Eng. 1 (2) (2004) 361.
[36] J.P. LaSalle, The Stability of Dynamical Systems, Society for Industrial and Applied Mathematics, Philadelphia, 1976.
[37] J.K.K. Asamoah, M.A. Owusu, Z. Jin, F.T. Oduro, A. Abidemi, E.O. Gyasi, Global stability and cost-effectiveness analysis of COVID-19 considering the impact of the environment: using data from Ghana, Chaos Solitons Fractals 140 (2020) 110103.
[38] J.O. Akanni, S. Olaniyi, F.O. Akinpelu, Global asymptotic dynamics of a nonlinear illicit drug use system, J. Appl. Math. Comput. (2020) 1–22.
[39] J.K.K. Asamoah, F. Nyabadza, Z. Jin, E. Bonyah, M.A. Khan, M.Y. Li, T. Hayat, Backward bifurcation and sensitivity analysis for bacterial meningitis transmission dynamics with a nonlinear recovery rate, Chaos Solitons Fractals 140 (2020) 110237.
[40] J. Wu, R. Dhingra, M. Gambhir, J.V. Remais, Sensitivity analysis of infectious disease models: methods, advances and their application, J. R. Soc. Interface 10 (86) (2013) 20121018, http://dx.doi.org/10.1098/rsif.2012.1018.
[41] E. Okyere, S. Olaniyi, E. Bonyah, Analysis of Zika virus dynamics with sexual transmission route using multiple optimal controls, Sci. Afr. 9 (2020) e00532.

[42] J.K.K. Asamoah, Z. Jin, G.-Q. Sun, B. Seidu, E. Yankson, A. Abidemi, F.T. Oduro, F. Alzahrani, S.E. Moore, E. Okyere, Sensitivity assessment and optimal economic evaluation of a new COVID-19 compartmental epidemic model with control interventions, Chaos Solitons Fractals (2021) 110885.
[43] J.K.K. Asamoah, Z. Jin, G.-Q. Sun, Non-seasonal and seasonal relapse model for Q fever disease with comprehensive cost-effectiveness analysis, Results Phys. 22 (2021) 103889.
[44] J.K.K. Asamoah, Z. Jin, G.-Q. Sun, M.Y. Li, A deterministic model for Q fever transmission dynamics within dairy cattle herds: Using sensitivity analysis and optimal controls, Comput. Math. Methods Med. 2020 (2020).
[45] W.H. Fleming, R.W. Rishel, Deterministic and Stochastic Optimal Control, Springer, New York, 1975.
[46] Ministry of Health Malaysia, Health facts 2014, 2019, URL http://www.moh.gov.my. (Accessed 15 March 2019).
[47] S. Lenhart, J.T. Workman, Optimal Control Applied to Biological Models, CRC Press, London, 2007.
[48] J.K.K. Asamoah, E. Okyere, A. Abidemi, S.E. Moore, G.-Q. Sun, Z. Jin, E. Acheampong, J.F. Gordon, Optimal control and comprehensive cost-effectiveness analysis for COVID-19, Results Phys. (2022) 105177.